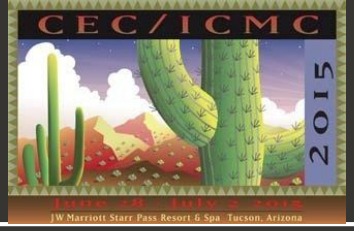

CEC/ICMC 2015
CRYOGENIC ENGINEERING CONFERENCE &
INTERNATIONAL CRYOGENIC MATERIALS CONFERENCE
JW Marriott Starr Pass Resort & Spa · Tucson, Arizona, USA
June 28 – July 2, 2015

Correlation of critical current density of bulk MgB_2 having high connectivity between SC grains with concentration and distribution of higher magnesium borides and oxygen-enriched inhomogeneities, the role of Ti additions

T. Prikhna [1], M. Eisterer [2], W. Goldacker [3], V. Sokolovsky [4], W. Gawalek [5], H.W. Weber [3], A. Kozyrev [1], V. Moshchil [1]

[1] *Institute for Superhard Materials of the National Academy of Sciences of Ukraine, Kiev 04074, Ukraine*

[2] *Atominstitut, Vienna University of Technology, Stadionallee 2, 1020 Wien, Austria*

[3] *Karlsruhe Institute of Technology (KIT), 76344 Eggenstein, Germany*

[4] *Ben-Gurion University of the Negev, P.O.B. 653, Beer-Sheva 84105 Israel*

[5] *Magnetworld AG, Buchaer Straße 6, 07745 Jena, Germany*

Introduction

Motivation

Critical current density, j_c, vs. magnetic field, $\mu_o H$, of MgB_2 materials synthesized at 2 GPa for 1 h from Mg+2B at 800 and 1050 °C;

From B (1) with grain size <5 μm, 0.66 wt% O, 0.31 wt% C, 0.48 wt% N, 0.32 wt % H

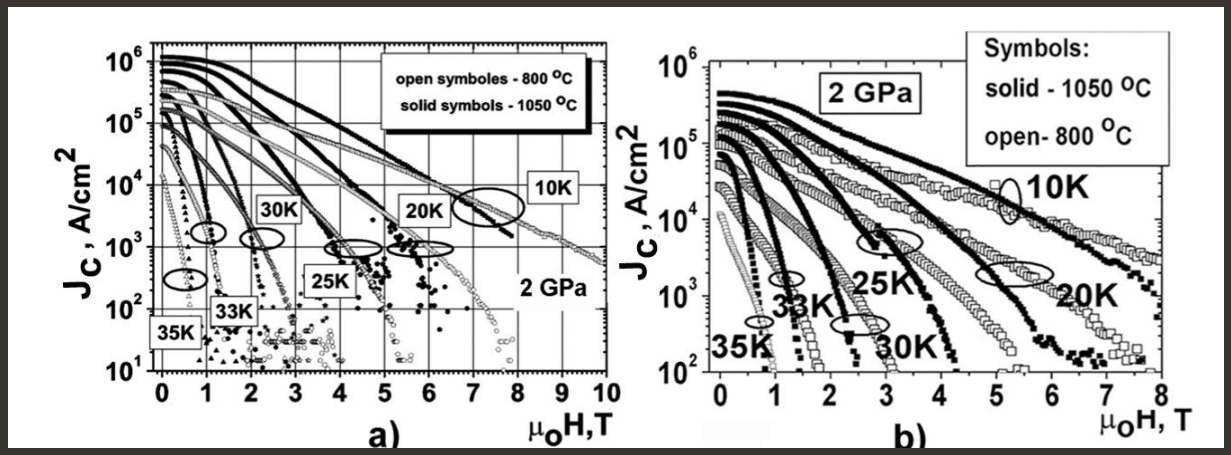

From B (2) with grain size 4 μm, 1.5 wt% O, 0.47 wt% C, 0.40 wt% N, 0.37 wt% H

j_c(0-1 T, 20 K)=0.9 – 0.7 MA/cm^2 j_c(0-1 T, 20 K)=0.4-0.3 MA/cm^2

From B(1) with 10 wt% SiC

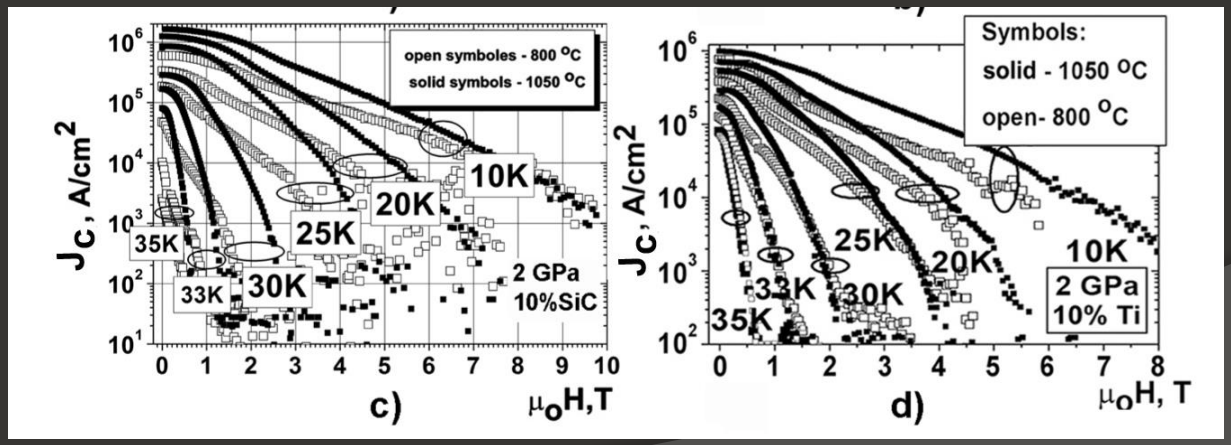

From B(2) with 10 wt% Ti

j_c(0-1 T, 20 K)=1.2 – 1.0 MA/cm^2 j_c(0-1 T, 20 K)=0.7-0.5 MA/cm^2

Introduction

B_{c2} (22 K)=15 T (No 1) and extrapolated B_{c2}(0 K)=42.1 T, as well, as irreversibility fields: B_{irr}(18.5 K)=15 T and B_{irr}(0 K)=32.5 T

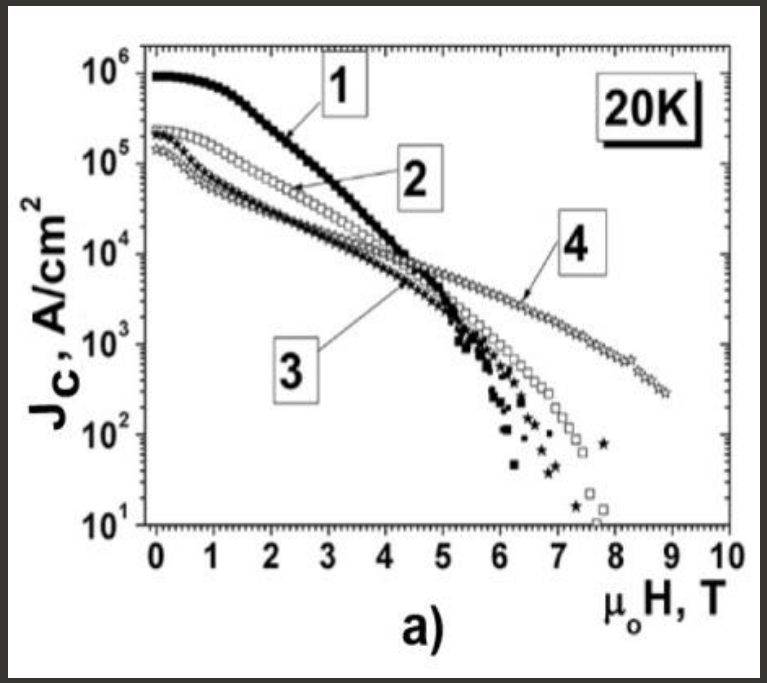

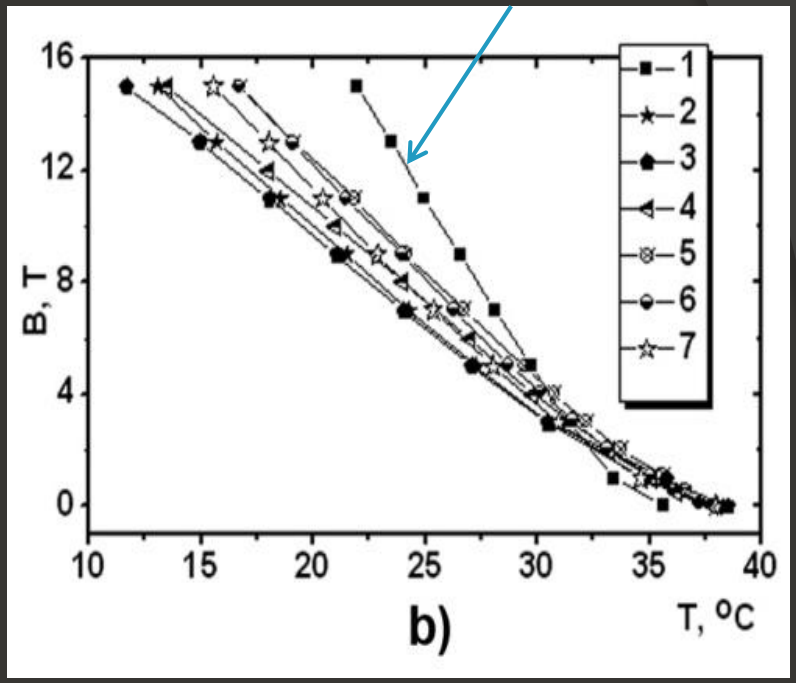

(a) Comparison of J_c at 20 K in bulk MgB_2 prepared under various temperatures at 2 GPa:
1, 2: samples made of B(I) at 1050 °C, (k=0.43) and 800 °C, (k=0.37), respectively;
3, 4 of B(II) at 800 °C and 600 °C, (k=0.32), respectively.

(b) B_{c2} of bulk MgB_2 prepared from Mg:2B :
1:B(II) at 2 GPa, 600 °C, 1 h, (HP);
2:B(III) at 30 MPa, 800 °C, 2h, (HotP);
3: B(III) at 50 MPa, 600-1050 °C, 1 h, (SPS);
4: B(III) at 2 GPa, 900 °C, 1 h (HP);
5:B(V)+10 wt.% Zr at 2 GPa, 800 °C, 1 h (HP);
6:B(V)+10 wt.% Ti at 2 GPa, 800 °C, 1 h (HP);
7:B(I)+10 wt.% SiC at 2 GPa, 1050 °C, 1 h (HP).

Pinning and j_c in MgB_2 can be influenced by:

- Material density
- Sizes of MgB_2 grains (due to intergrain boundaries can be pinning centers and higher surface area of grain boundaries is preferable)
- Connectivity between SC grains
- Shielding fraction (correlates with amount of SC phase)
- Presence of inclusions of secondary phases with different (from MgB_2) Tc or nonsuperconductive (sizes of pinning centers should be commensurable with coherence length in MgB_2)
- Dopants which can be introduced into MgB_2 lattice and cause lattice distortion (carbon)

Methods of preparation

SPS = Spark plasma sintering 16-96 MPa

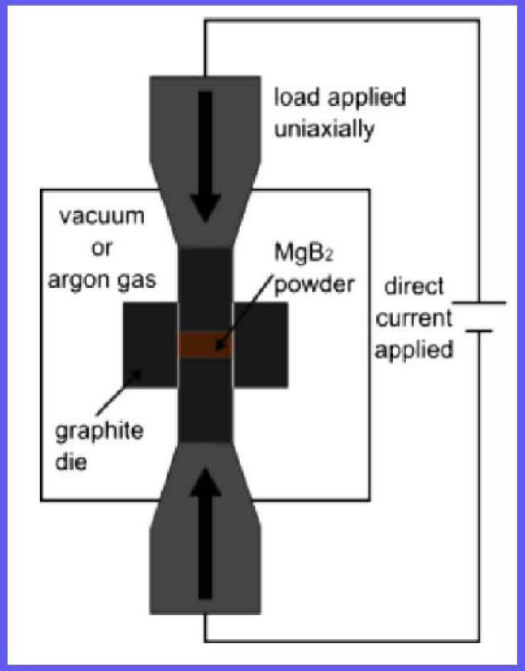

Scheme of SPS-system

7

Hot – P = Hot-pressing
30 MPa (300 atm)

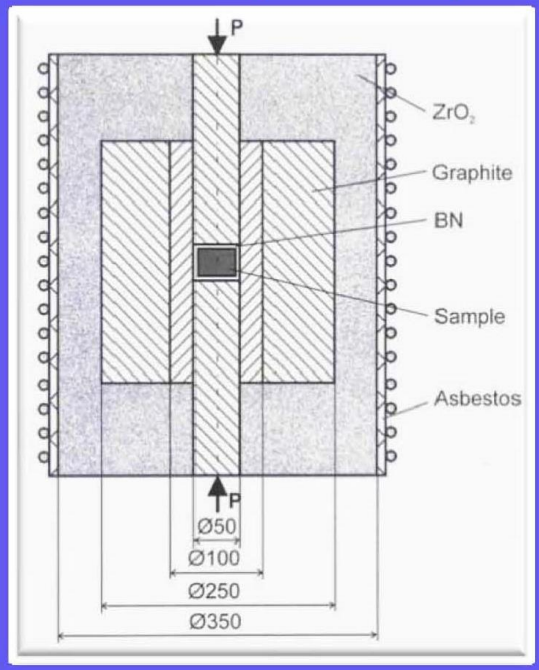

Possibility to press blocks up to 200 mm in diameter

(in cooperation with Dr. J. Noudem, CRISMAT, Caen, France)

Methods of preparation

ASEA (Swedish industry Company Allmänna Svenska Elektriska Aktiebolaget)

High pressure – high temperature
2 GPa, 1050 ^{o}C, 1 h

MgB_2 items up to 150 mm in diameter

14 000-ton press
140 MN effort

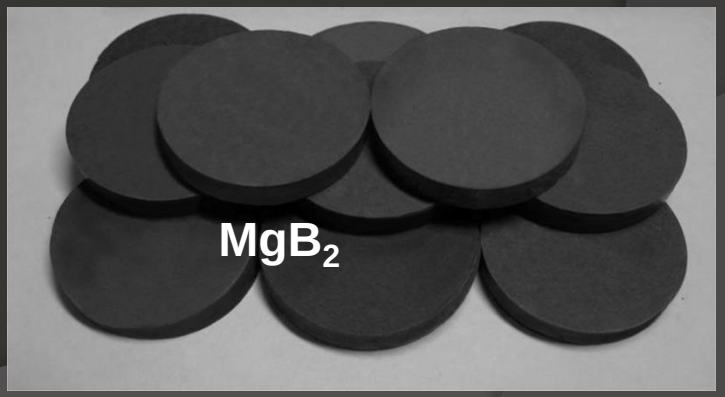

Methods of preparation
Cube type high pressure apparatus

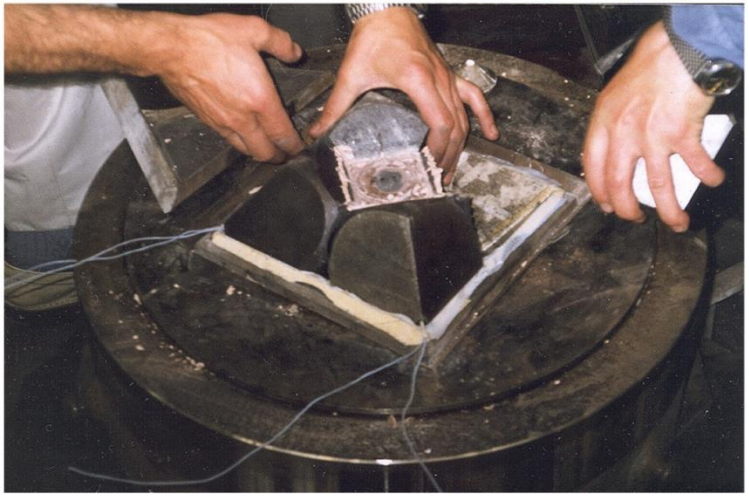

The scheme of reaction cell of the cube type high pressure apparatus.

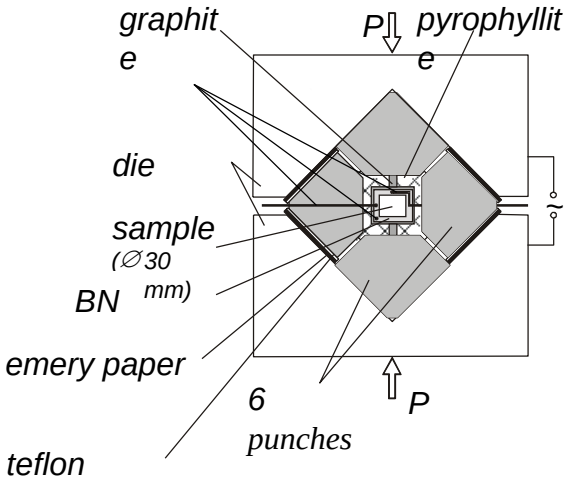

Scheme of load distribution

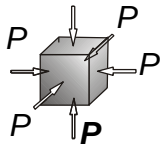

Methods of preparation

The recessed-anvil type high pressure apparatus with working volume 330 cm^3 (under 2 GPa pressure)

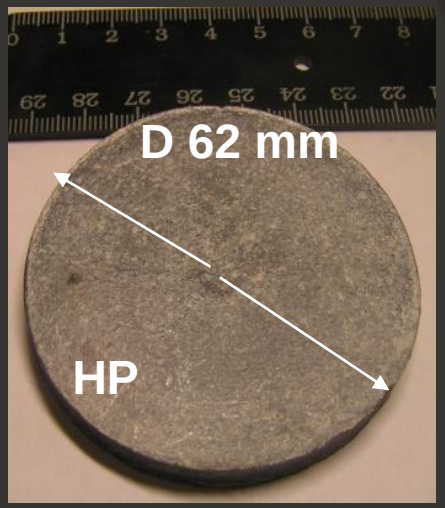

HPA for manufacturing blocks up to 150 mm in diameter

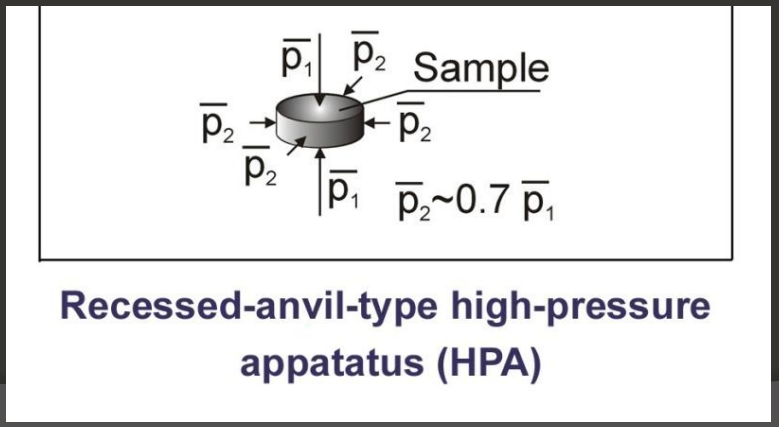

Recessed-anvil-type high-pressure appatatus (HPA)

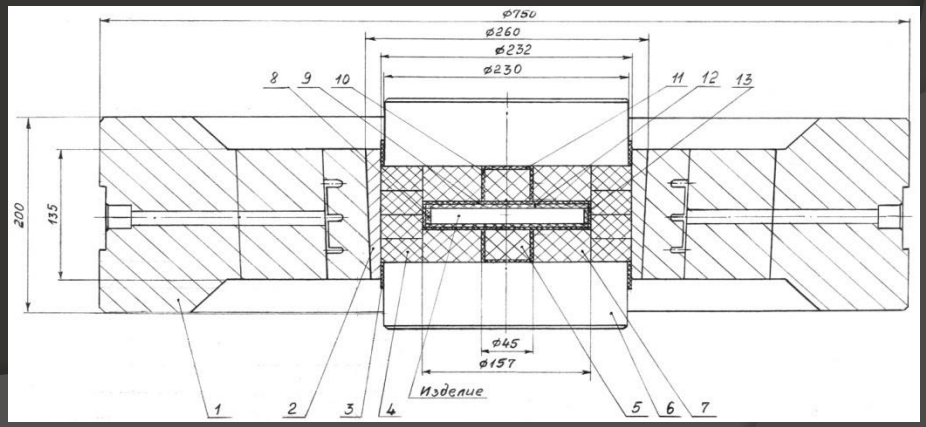

HPA cylinder-piston(V_p= 6300 cm^3) P=1-2 GPa, T =600-1100 °C, Press ASEA 140 MN effort

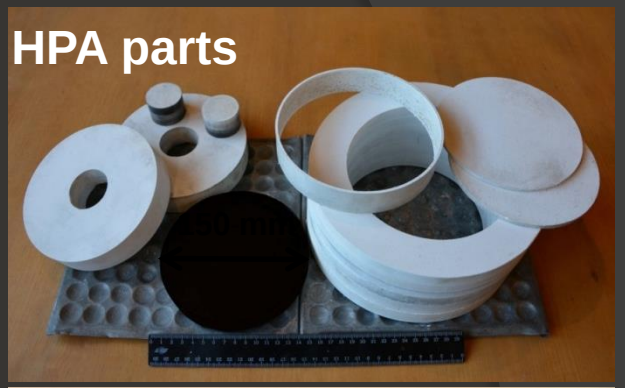

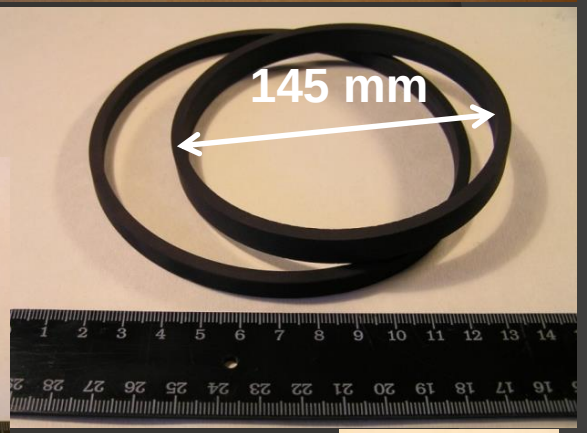

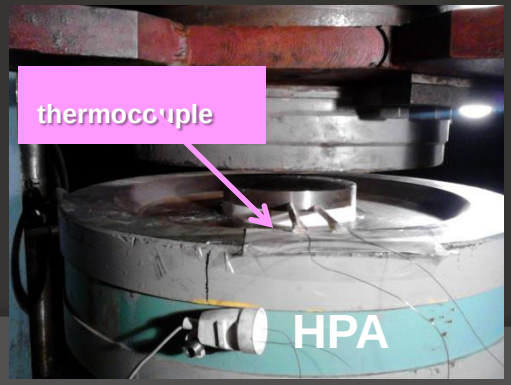

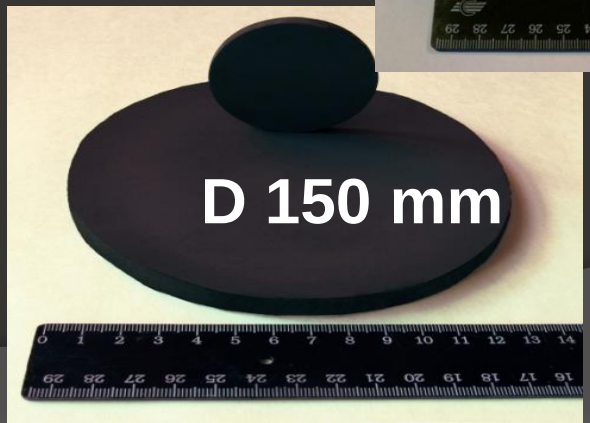

Items from MgB_2

MgB_2-based superconductors

working temperature 20-30 K

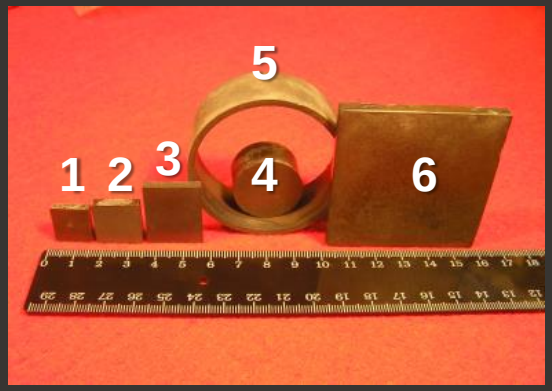

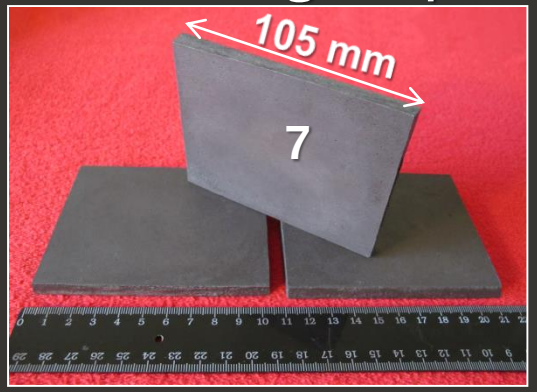

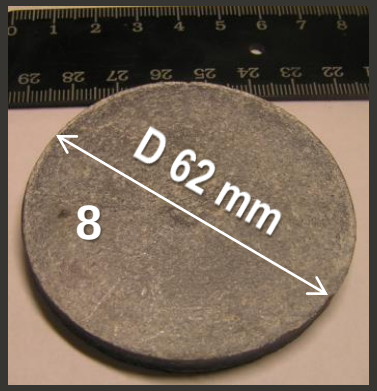

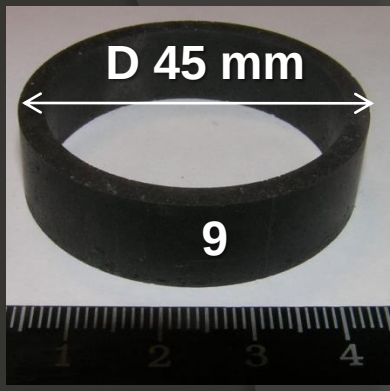

1-4, 8, 9 - High pressed (2 GPa); 5 – HIP (0.1 GPa); 7- Hot Pr. (30 MPa)

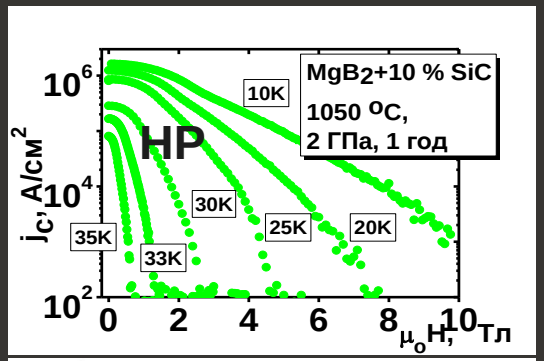

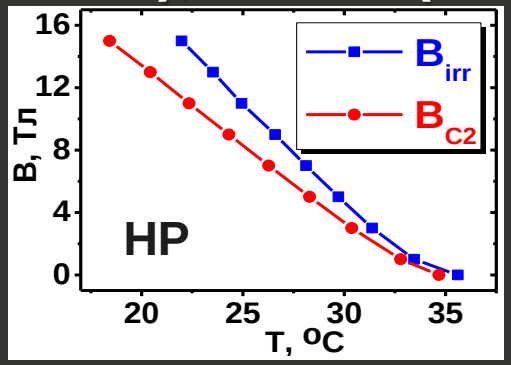

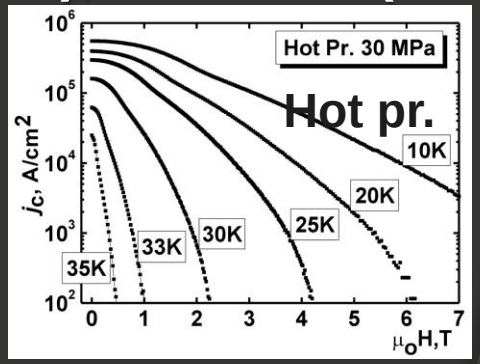

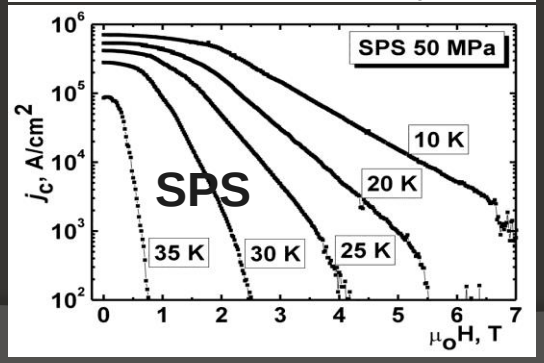

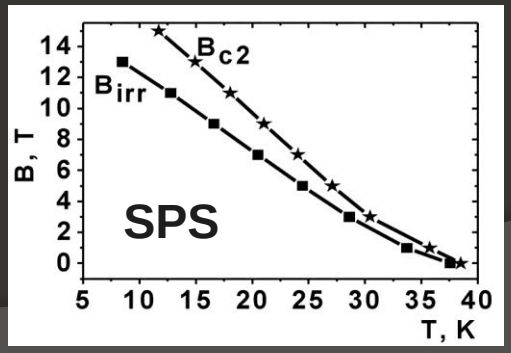

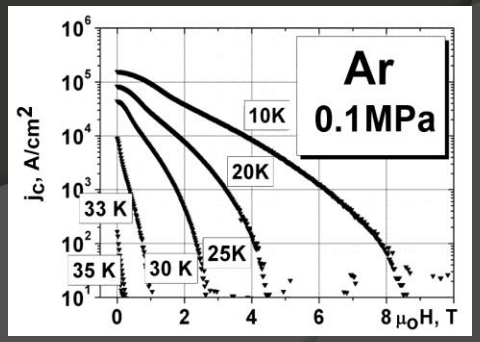

High-pressure (2 GPa, 800 °C, 1 h) treated wire from MgB_2

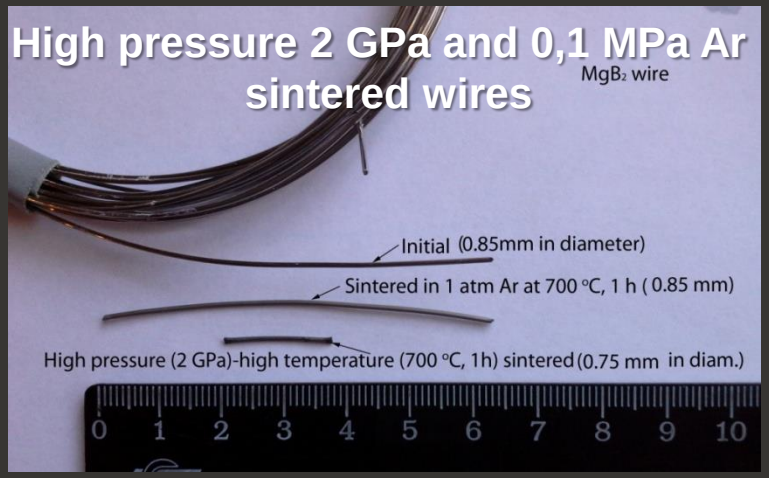

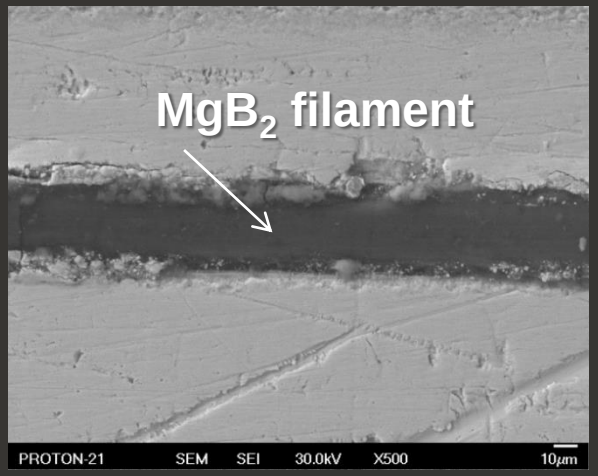

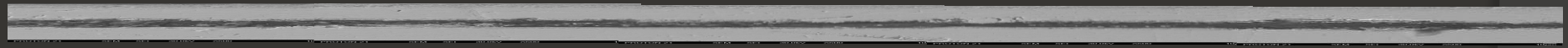

Panorama of MgB_2 filament after high pressure-high temperature treatment

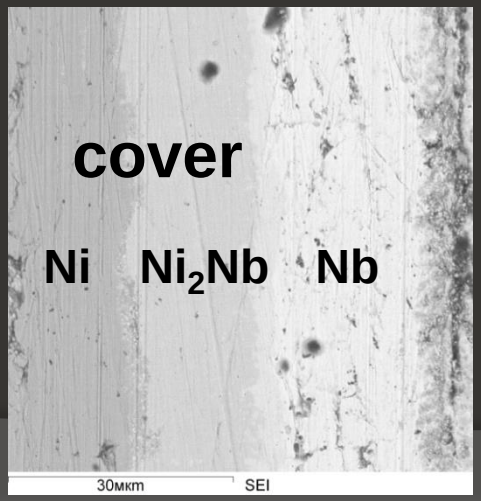

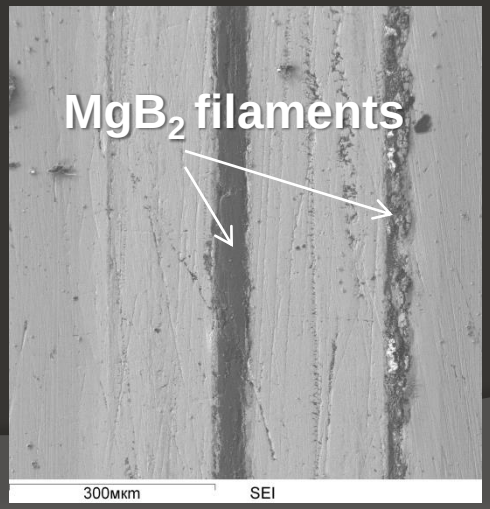

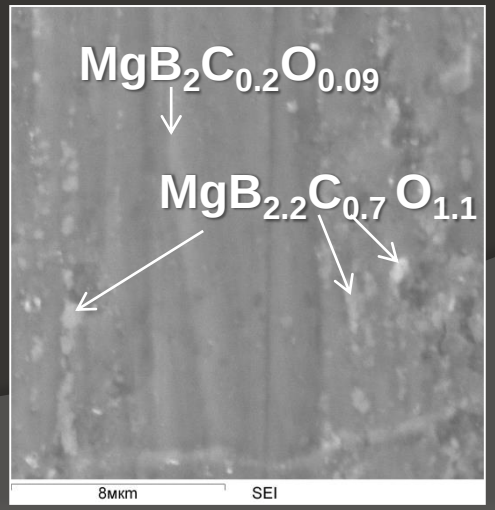

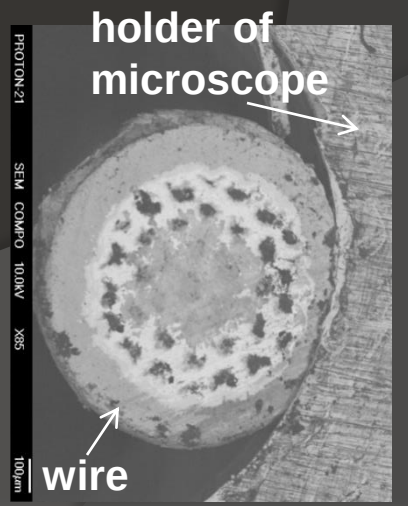

Estimation of MgB_2 density

Table 2. Characteristics (critical current density-j_c, maximal pinning force-$F_{p(max)}$, amount of MgB_2, MgO and MgB_4 estimated from Rietveld refinements, and density-ρ) of MgB_2-based materials prepared under different *P-T* conditions from Mg and B taken in MgB_2 stoichiometry or from MgB_2 powder using different methods: under high quasihydro-static pressure –HP, by hot pressing HotP, by spark plasma sintering – SPS, by pressureless sintering under 0.1 MPa of Ar – PL.

No	Preparation	Type of B	*P*, MPa	*T*, °C	j_c, MA/cm^2, at 0-1 T, at 20 K	$F_{p(max)}$/ 10^9(N/m^3) at 20 K	MgB_2/MgO/ MgB_4, wt%	Den-sity, ρ
1.	in-situ, HP	I	2000	1050	0.9 – 0.7	7.6	94/6/0	99%
2.	in-situ, HP	I	2000	800	0.2 – 0.15	1.6	91/5.5/0	98%
3.	in-situ, HP	III	2000	1050	0.4 – 0.3	2.3	87/13/0	99%
4.	in-situ, HP	III	2000	1000	0.36-0.23	2.4	86/14/0	99%
5.	in-situ, HP	III	2000	950	0.3 – 0.2	2.1	-	98%
6.	in-situ, HP	III	2000	900	0.12 – 0.06	1.1	71/13/0	98%
7.	in-situ, HP	III	2000	800	0.12 – 0.07	0.8	73/12/0	97%
8.	in-situ, HP	II	2000	600	0.14 – 0.05	0.6	64/30/0	83%
9.	in-situ, SPS	III	50	1050	0.5 – 0.4	4.6	83/4.5/12.5	94%
10.	in-situ, SPS	III	50	800	0.4 – 0.36	2.7	-	74%
11.	ex-situ, SPS	-	50	1050	0.4 – 0.3	3.3	83/6.5/10.5	96%
12.	in-situ, HotP	III	30	1050	0.08 – 0.016	0.2	46/8.5/45.5	99%
13.	in-situ, HotP	III	30	800	0.3-0.2	0.6	-	72%
14.	in-situ, PL	IV	0.1	800	0.08-0.03	1.9	90/10/0	55%
15.	in-situ, cold dens. 2 GPa, PL	III	0.1	600	0.26-0.13	1.3	94.5/5.5/0	65%

Estimation of grain sizes in MgB_2

The average crystallite sizes were calculated from line broadening in X-ray diffraction pattern by the standard program in accordance with the following:

$$\text{Crystallite size} = \frac{K \cdot \lambda}{W_{\text{size}} \cdot \cos\theta} \quad \text{with} \quad W_{\text{size}} = W_{\text{b}} - W_{\text{s}}$$

where W_{size} is the broadening caused by small crystallites; W_b is the broadened profile width; W_s is the standard profile width (0.08 °); K is the form factor; λ is the wavelength.

Table. Critical current density, j_c, vs. relative average grain size of crystallites of high-pressure sintered from MgB_2 and synthesized from Mg and B taken in1:2 ratio materials

High pressed at 2 GPa for 1 h at T_s, °C	average crystal sizes	lattice parameters		j_c, kA/cm^2 at 10 K		j_c, kA/cm^2 at 20 K	
		a (nm)	*c* (nm)	0 T	1 T	0 T	1 T
From MgB_2 (10 μm and 0.8 % of O)							
700	19.7 nm	0.30805	0.35188	-	-	-	-
800	18.8 nm	0.30822	0.35212	-	-	-	-
900	18.5 nm	0.30820	0.35208	56	14	36	8
1000	25.0 nm	0.30797	0.35200	28	8	19	5
From Mg chips and B (4 μm, 1.5 % O) mixed and milled in 1:2 ratio							
800	15.0 nm	0.30747	0.35188	245	142	138	79
900	21.0 nm	0.30819	0.35174	205	136	128	61
1000	37.0 nm	0.30808	0.35192	485	364	360	237

Estimation of connectivity, A_F

$$A_F = \frac{9\ \mu\Omega\cdot\mathrm{cm}}{\rho_{300} - \rho_{40}}$$

$$9\ \mu\Omega\cdot\mathrm{cm}$$

perfect connectivity for MgB_2

resistivity $\rho = \dfrac{V\cdot\sigma}{I\cdot\Delta l}$

$$\rho_{300} = \frac{V_{300}\cdot\sigma}{I\cdot\Delta l} \qquad \rho_{40} = \frac{V_{40}\cdot\sigma}{I\cdot\Delta l}$$

Δl - distance between voltage contacts

$\sigma = a\cdot b$ - cross-section area of the sample, $a\cdot b\cdot c$ - sample dimensions

V_{300} - arithmetic average of all V data at room temperature

V_{40} – voltage at 40 K

I =100 mA - current

ρ - by four probe method

Estimation of pinning mechanism

M. Eisterer " Calculation of the volume pinning force in MgB_2 superconductors" (PHYSICAL REVIEW B 77, 144524 2008)

Identification of the dominant pinning mechanism from the peak position of pinning volume force:

$$k = B_{peak}/B_n ;$$

$$B_{peak} - F_{p(max)}, \quad B_n - F_{p(max)}/2$$

The dominant pinning mechanism was determined from the volume pinning force j_cB according to a scaling procedure proposed by M.Eisterer , which eliminates the influence of the intrinsic anisotropy of MgB_2 on the field dependence of the volume pinning force. The field B_{peak}, where the maximum of the volume pinning force occurs, was normalized by the field B_n, at which the volume pinning force drops to half its maximum (on the high field side), instead of the upper critical field, B_{c2}, in the original approach for isotropic superconductors . For typical values for the anisotropy (4) and the percolation threshold (0.25) in bulk MgB_2 samples, the position of the peak, B_{peak}/B_n, is expected to be at 0.34 and 0.47 for grain boundary and point pinning, respectively. Changes in the anisotropy and the percolation threshold only slightly change the peak position, in particular in the realistic range of these parameters. Another advantage of this scaling approach is that B_n is easily available and no separate experiment for determining B_{c2} or any extrapolation to estimate the irreversibility (or Kramer) field is necessary to define the scaling field.

Estimation of connectivity, A_F, amount of shielding fraction, S, and type of pinning, k.

Connectivity, A_F, k-ratio: $k = B_{peak}/B_n$ and amount of shielding fraction, S, of MgB_2 materials prepared under different conditions. The numbering in tables 1 and 2 is the same.

No	Preparation	Type of B	P, MPa	T, °C	$k = B_{peak}/B_n$	A_F, %	S, %
1.	in-situ, HP	I	2000	1050	0.43	-	-
2.	in-situ, HP	I	2000	800	0.37	-	-
3.	in-situ, HP	III	2000	1050		79	94
5.	in-situ, HP	III	2000	950	-	59	81
7.	in-situ, HP	III	2000	800		57	91-100
8.	in-situ, HP	II	2000	600	0.32	18	90
9.	in-situ, SPS	III	50	1050	-	98	91
11.	ex-situ, SPS	-	30	1050	-	80	100
12.	in-situ, HotP	III	30	1050	-	32	-
13.	in-situ, HotP	III	30	800	-	73	-
15.	in-situ, cold dens. 2 GPa, PL	III	0.1	600	-	-	75
16.	in-situ, cold dens. 2 GPa, PL	III	0.1	800	-	-	84

With synthesis temperature increase the shift from grain boundary pinning towards point pinning occurs (about what k-ration increase witnessed)

CONTRADICTIONS BETWEEN X-RAY DATA AND SEM OBSERVATIONS

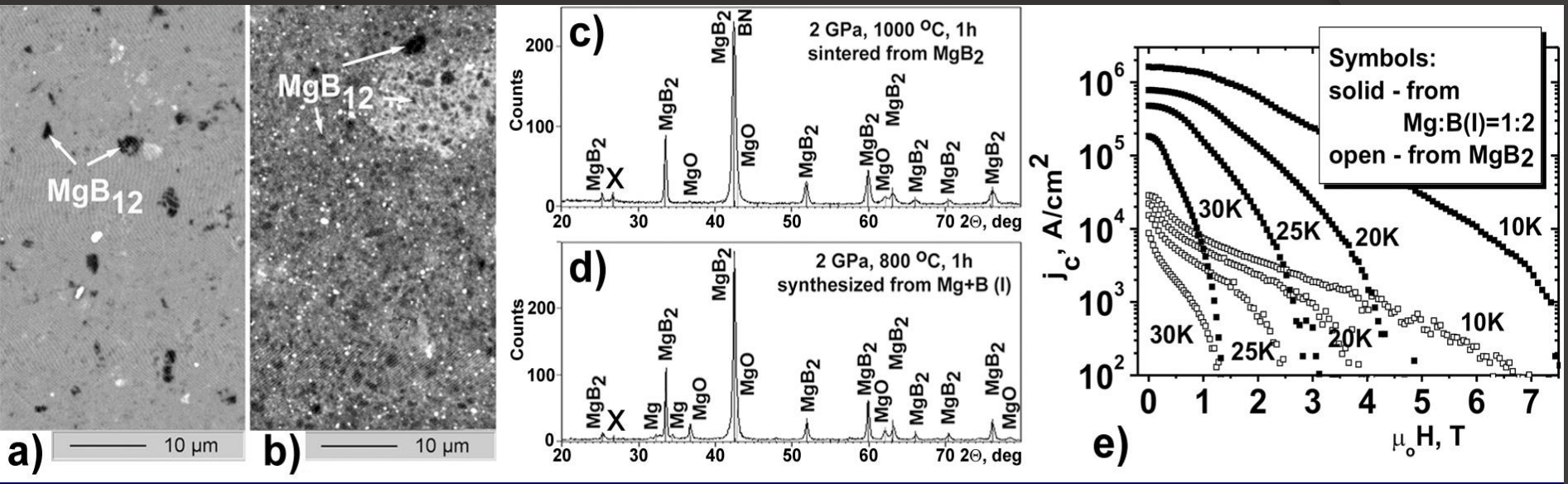

(a), (b) structures of the samples obtained by SEM in COMPOsitional contrast:
(a) sintered from MgB_2 at 2 GPa, 1000 °C, 1 h;
(b) synthesized from Mg and B taken into 1:2 ratio at 2 GPa, 800 °C, 1 h;
(c), (d) –X-ray patterns of the samples shown in Figs. 5a, b;
(e) dependences of critical current density, j_c, on magnetic fields, $\mu_o H$, at different temperatures of the samples shown in Fig. e: open symbols – sintered from MgB_2 material and solid symbols - synthesized from Mg and B taken in 1:2 ratio

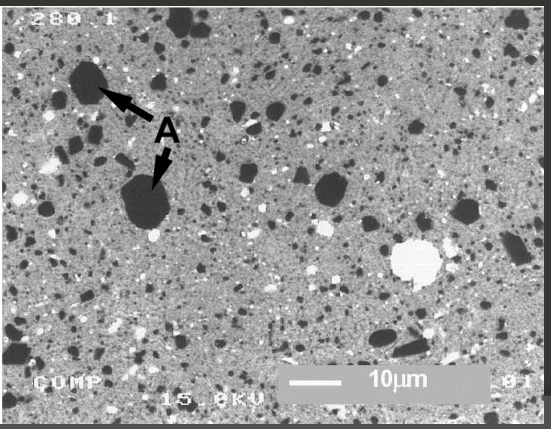

Structure of MgB_2-based material synthesized from amorphous boron and magnesium chips taken in Mg:B=1:2 ratio in contact with Ta foil at 2GPa, 800°C, 1h (BEI SEM image) shows that inclusions of black phase with near MgB_{12} stoichiometry may crystallize in hexagonal habit or have near hexagonal cross-section (see, for example, inclusion marked "A")

Each of the following non-superconducting higher magnesium borides in the Mg-B system can crystallize in the MgB_2 matrix and can influence pinning

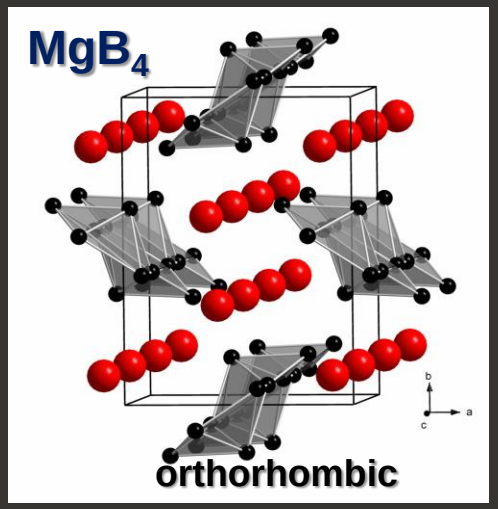

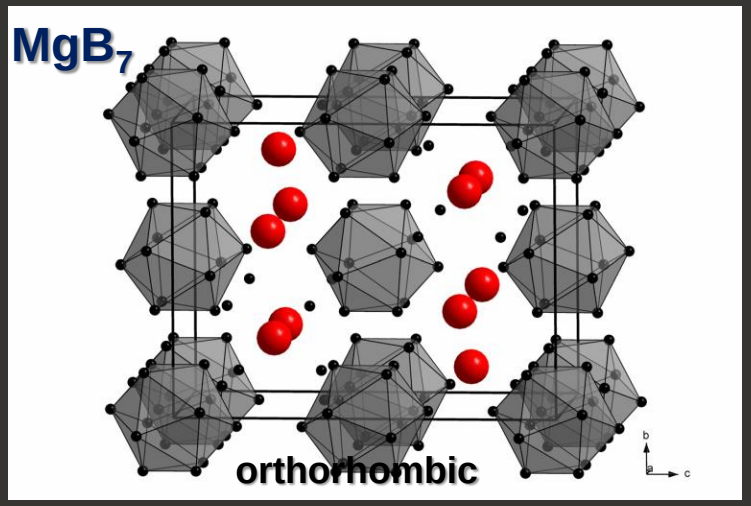

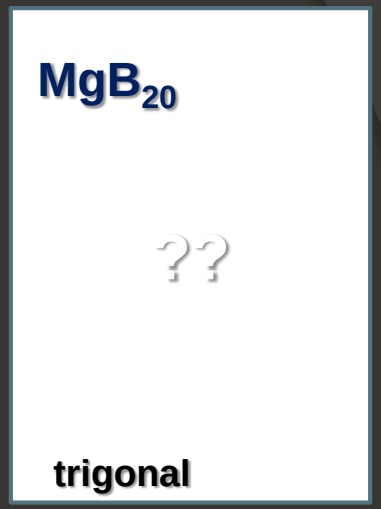

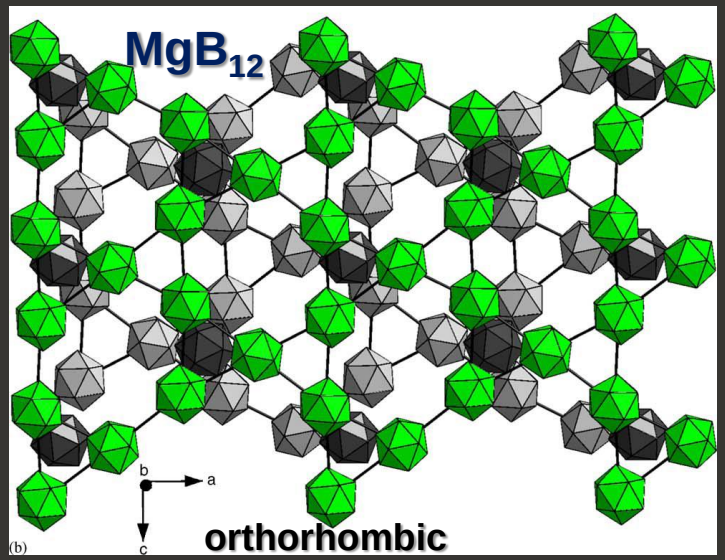

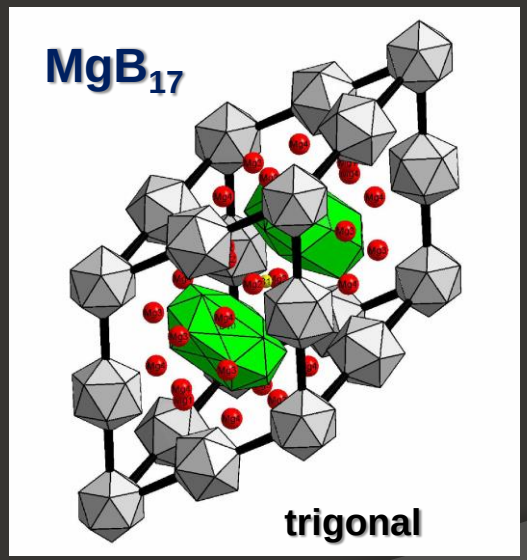

The method of preparation (pressure-temperature-time conditions) can affect the stoichiometry of the MgB_x inclusions in MgB_2. (2 GPa – MgB_{12})

The size and amount of higher magnesium borides (black inclusions with near $MgB_{11-13}O_{0.2-0.3}$ stoichiometry according to Auger study) decreasing with manufacturing temperature increase

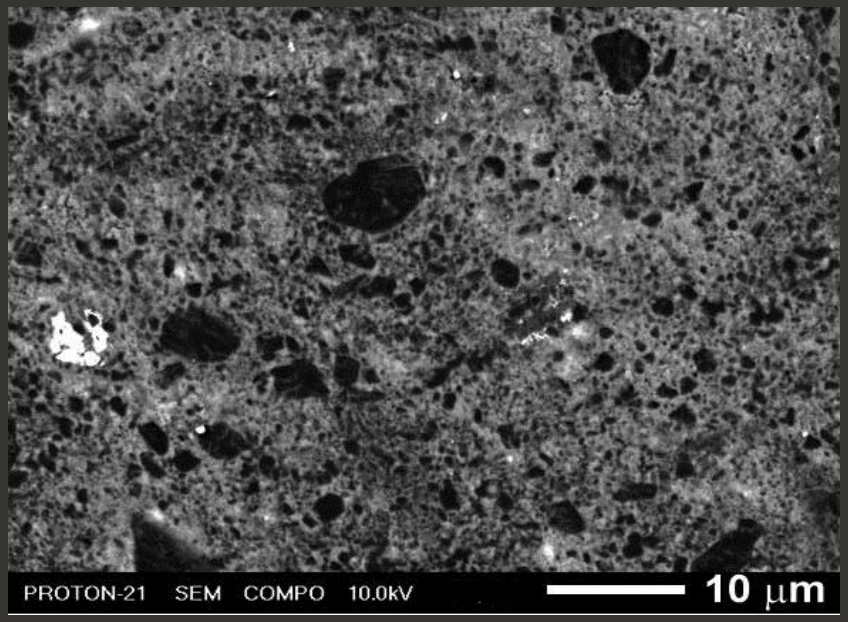

Mg:2B, 2 GPa, 800 °C, 1 h

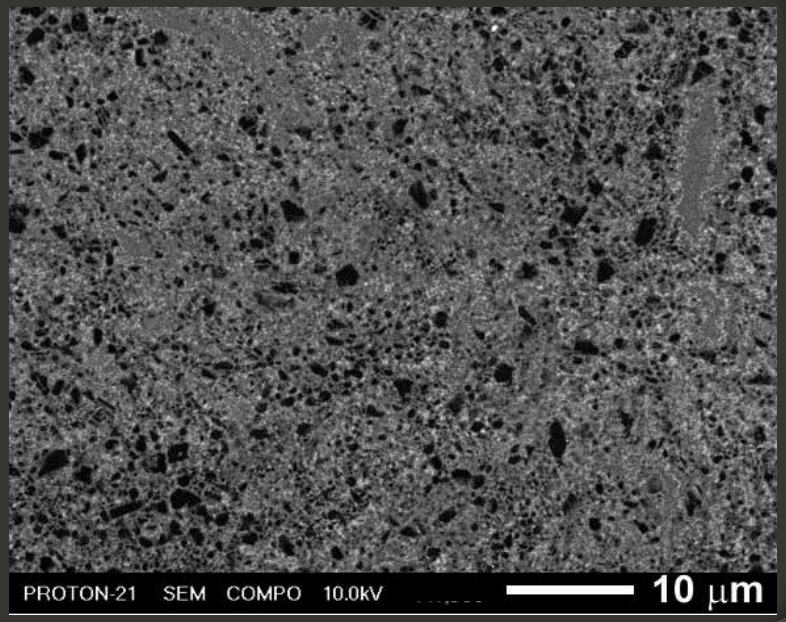

Mg:2B, 2 GPa, 1050 °C, 1 h

The Berkovich nanohardnes and Young modulus of such inclusions as estimated under the 10-60 mn-load were 32.2±1.7 and 385±14 GPa, respectively, what were even higher than that for sapphire: 31.1±2.0 and 416±22 GPa.

Typical structures of MgB_2 prepared at 0.1 MPa – 2 GPa at low temperatures (a) - 600-800 °C and high (b) -1000-1100 °C and their compositions

0.1 MPa – 2 GPa

a)

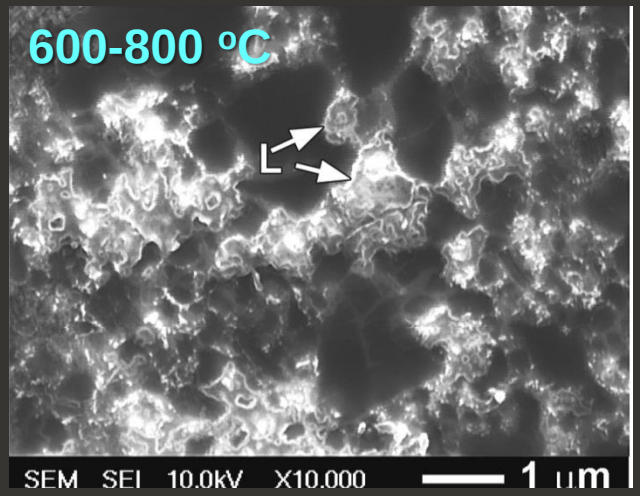

b)

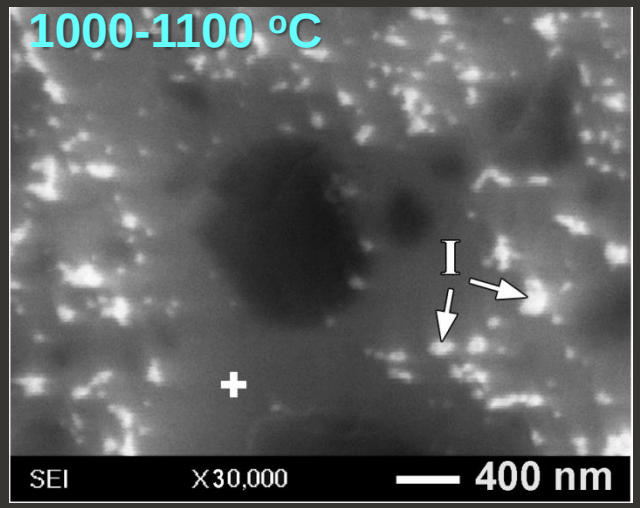

"*L* " - $MgB_{0.9\text{-}3.5}O_{1.6\text{-}2}$ white layers, thickness (15-20 nm)

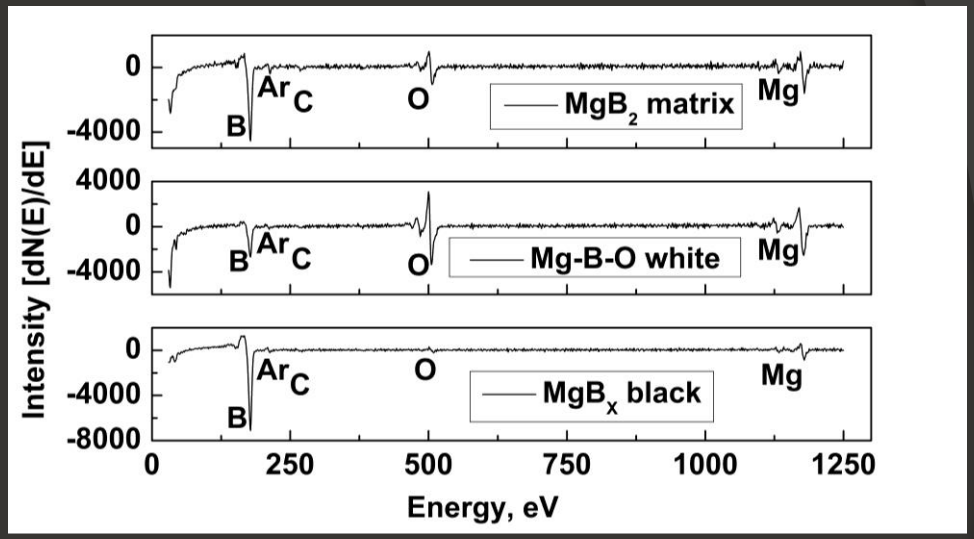

Auger spectrum

"*I*" - $MgB_{0.5\text{-}0.8}O_{0.8\text{-}0.9}$ white inclusions

$MgB_{11\text{-}13}O_{0.2\text{-}0.5}$ black inclusions

$MgB_{2.2\text{-}1.7}O_{0.3\text{-}0.6}$ gray matrix.

Auger study by JAMP–9500F

Zone of excitation being 10 nm in diameter and two lattice parameters in depth etching in Ar allows to exclude analyzing of oxidized layer on the surface!

Auger study by JAMP−9500F

zone of excitation being 10 nm in diameter and two lattice parameters in depth

Mg(I):2B(III), 1200 °C, 2 GPa, 1h

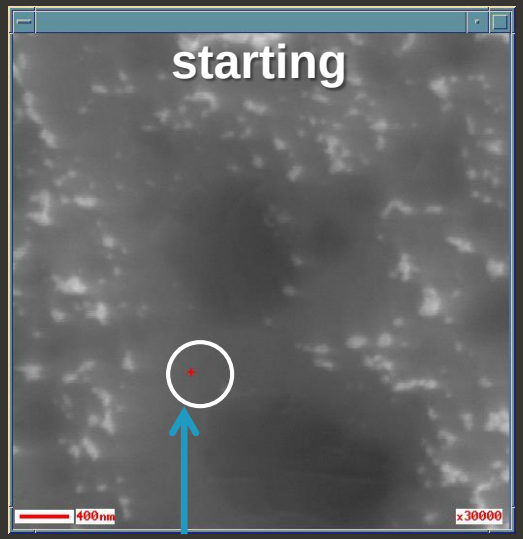

Place of analysis

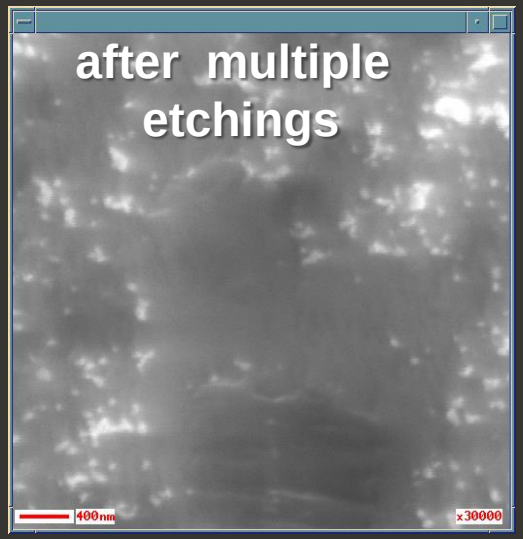

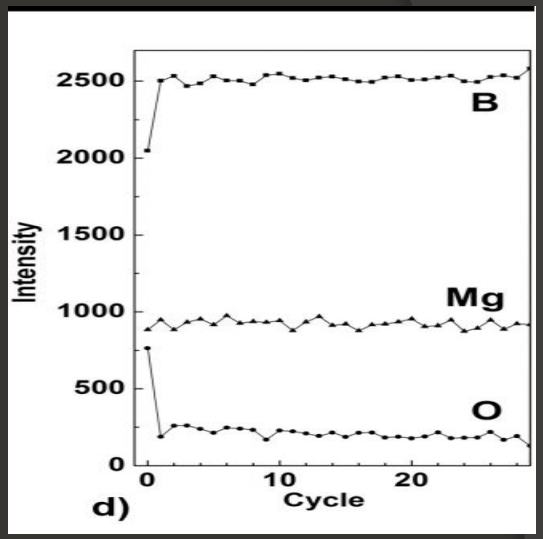

Spectrums of gray matrix

Depth profile of gray matrix

$MgB_{0.5\text{-}0.8}O_{0.8\text{-}0.9}$ white inclusions
$MgB_{11\text{-}13}O_{0.2\text{-}0.5}$ black inclusions
$MgB_{2.2\text{-}1.7}O_{0.3\text{-}0.6}$ gray matrix.

Comparing these results with that of X-ray structure analysis we can conclude that boron incorporated into the MgB_2 structure.
Repeated etching in Ar (in the JAMP−9500F chamber during study) and quantitative Auger analysis showed practically the same oxygen concentration in MgB_2 matrix of the structure after 30 cycles, which points to the oxygen incorporation into the MgB_2 lattice.

$Mg(B,O)_2$ precipitation in MgB_2 (X. Z. Liao et al. J. Appl. Phys. 93, 6208 (2003)

(a) An HREM image along [010] direction.

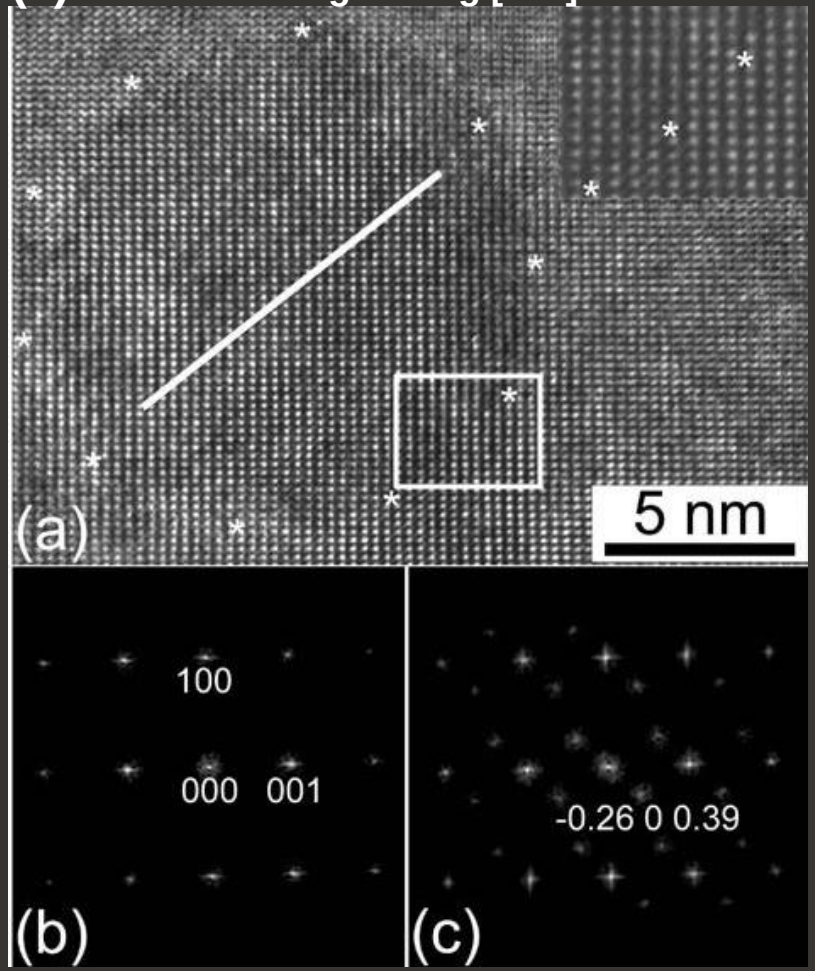

(b) Fourier transformation of the matrix.

(c) Fourier transformation of the precipitate showing satellite spots with a vector of [-0.26, 0, 0.39]

MgB_2 grains to form coherently ordered $MgB_{2-x}O_x$ precipitates from about 5 up to 100 nm in size and that such precipitates can act as pinning centers

Ordered replacement of B atoms by O and have the same basic structure as the MgB_2 matrix but with composition modulations.

No difference in the lattice parameters between the precipitates and the matrix can be detected in conventional electron diffraction patterns.

However, extra satellite diffraction spots were revealed by HREM study in some directions implying a structural modulation caused by the precipitates.

The periodicity of O atom ordering depends on the concentration of O atoms in the precipitate and primarily occurred in the (010) plane.

$Mg(B,O)_2$ precipitation in MgB_2 (X. Z. Liao et al. J. Appl. Phys. 93, 6208 (2003)

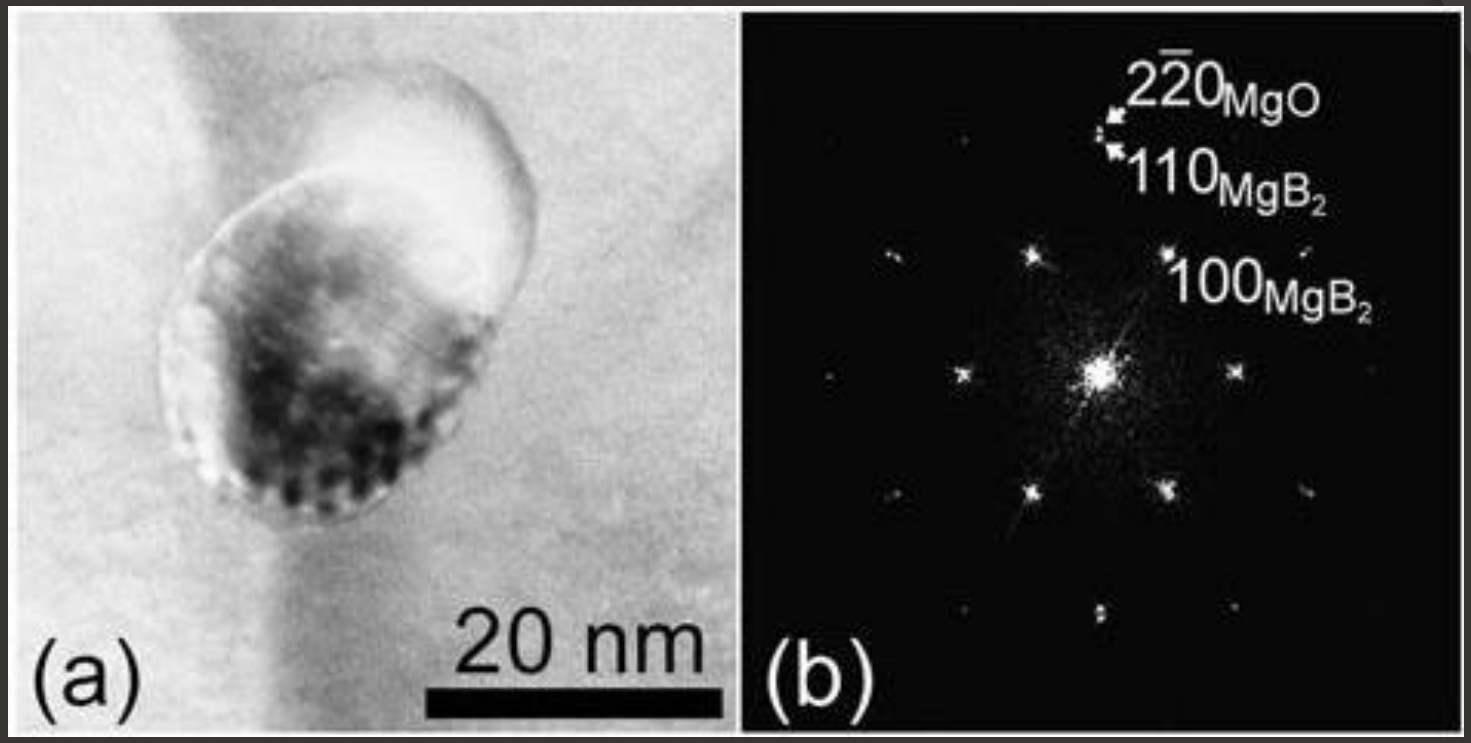

Longer exposure to trace amount of O at high temperatures also results in the transformation of the precipitates from the hexagonal $Mg(B,O)_2$ phase with compositional modulations to the face-centered cubic MgO phase, implying $Mg(B,O)_2$ is not a stable phase at high temperature in an environment containing trace amount of oxygen. The orientation relationship between the resulting MgO precipitates and the MgB_2 matrix revealed by an HREM image and its Fourier transformation in Fig. is: $[001]MgB_2$ //[111]MgO, and $(110)MgB_2$//(1-10)MgO (note that planar distance $d(110)MgB_2$ = 0.154 nm while d(220)MgO = 0.149 nm. The lattice mismatch between $d(110)MgB_2$ and d(220)MgO is only 3.2%).

Increase of j_c in low and medium magnetic fields with increase of manufacturing temperature and effect of Ti addition

2 GPa, 1 h

from Mg:2B

from Mg:2B + 10% Ti

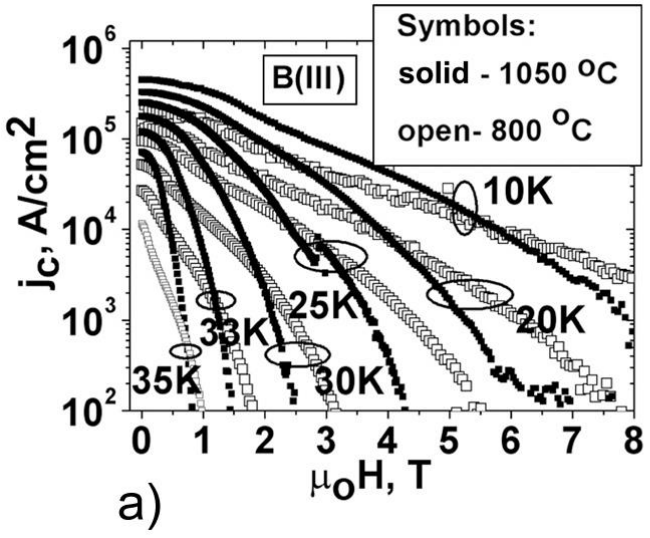

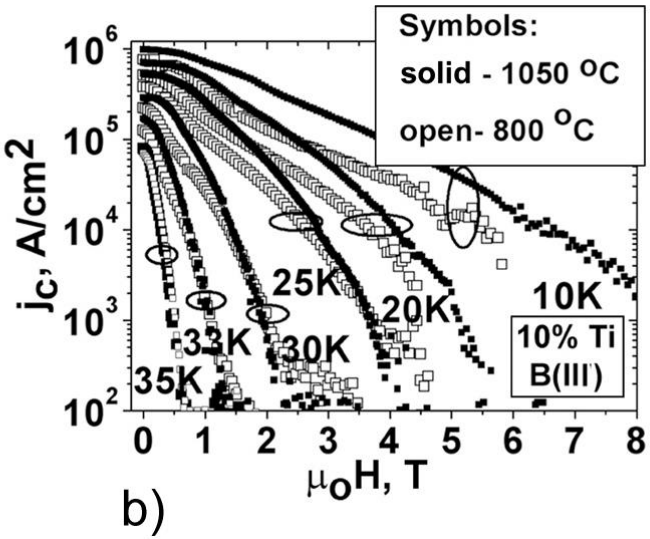

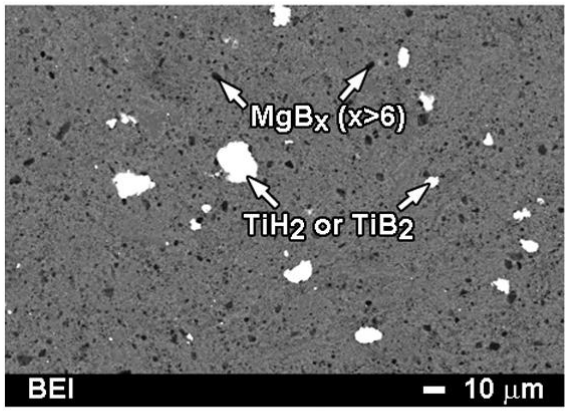

Boron amorphous: grain size 4 μm, 1.5 wt% O, 0.47 wt% C, 0.40 wt% N, 0.37 wt% H

- **The critical current density of MgB_2 – based materials usually increases at low and medium magnetic fields with increasing manufacturing temperature, but lower manufacturing temperatures can result in a j_c increase at high magnetic fields.**
- **A shift from grain boundary pinning to point pinning was observed**
- **A positive effect in enhancing the critical currents of MgB_2 is played,, by dopants, such as Ti, for example.**

X-ray diffraction patterns of the materials prepared from Mg:2B under 2 GPa for 1 h without additions at 800 °C (a) and 1050 °C (b) and with 10 wt. % Ti at 800 °C (c) and 1050 °C (d).

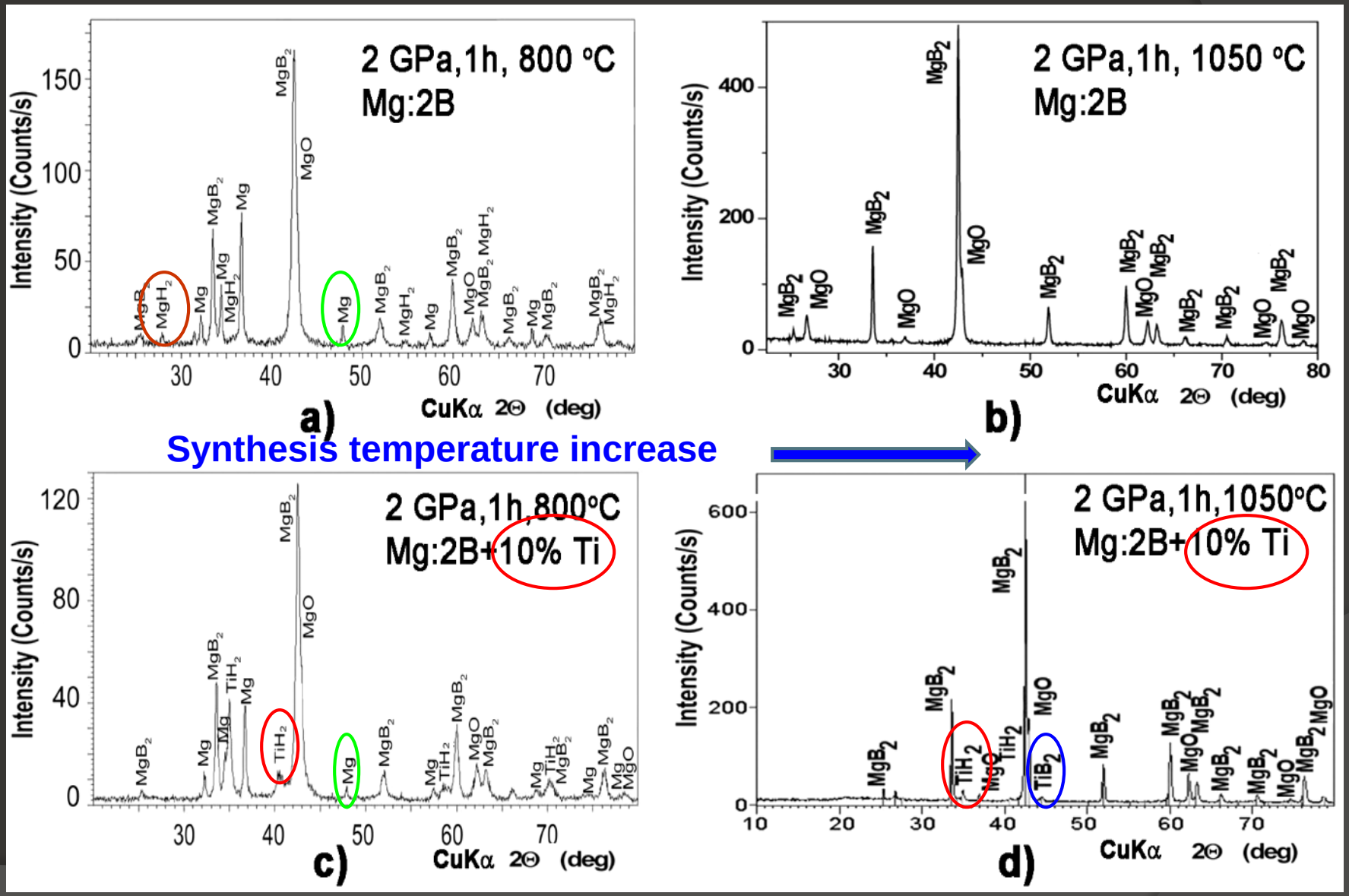

Mg:2B + TiH_2 (10 wt.%) 2 GPa, 950 °C, 1 h

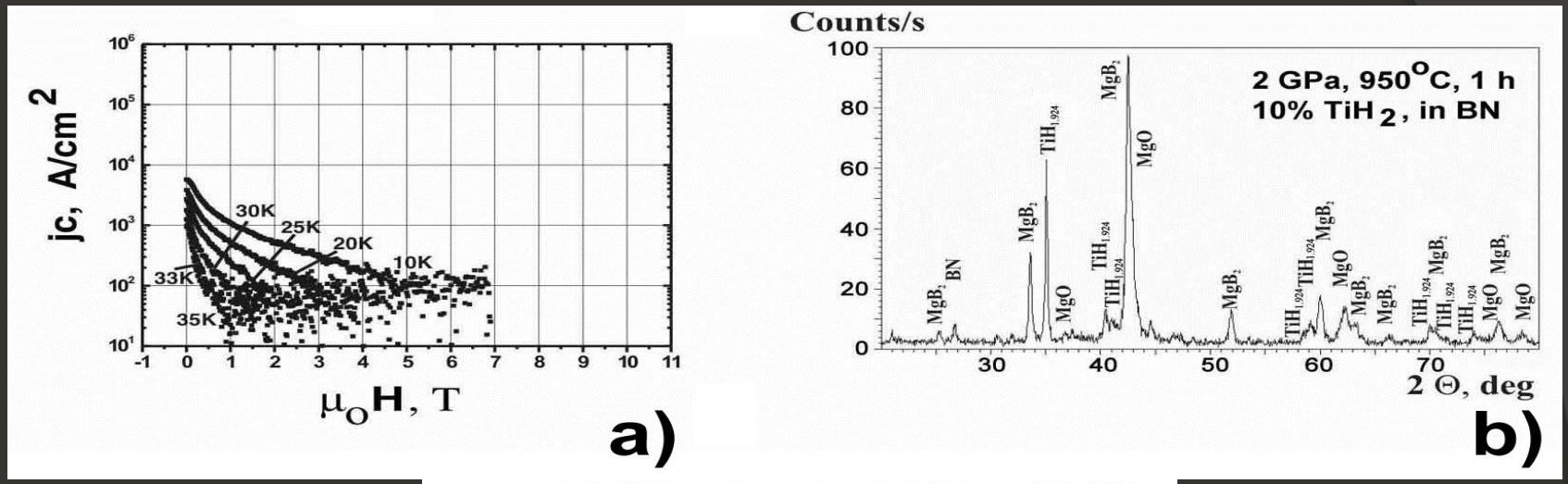

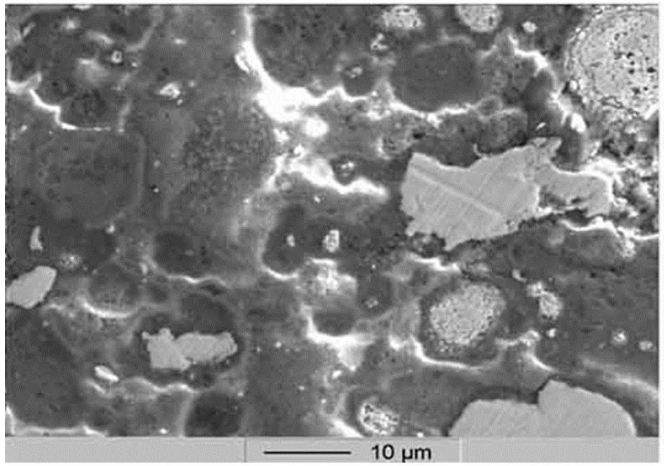

(a) Dependences of J_c on μ_oH, of the high-pressure synthesized MgB_2 –based materials from Mg:B=1:2 + 10 wt % TiH_2; at 2 GPa, 950 °C, 1 h; (b) X-ray pattern of the sample; (c) structure of the sample obtained by SEM (c) SEI (secondary electron image)

S. Haigh, P. Kovac, T. A. Prikhna, C. Grovenor, Supercond. Sci. Technol. 18, 1190 (2005).

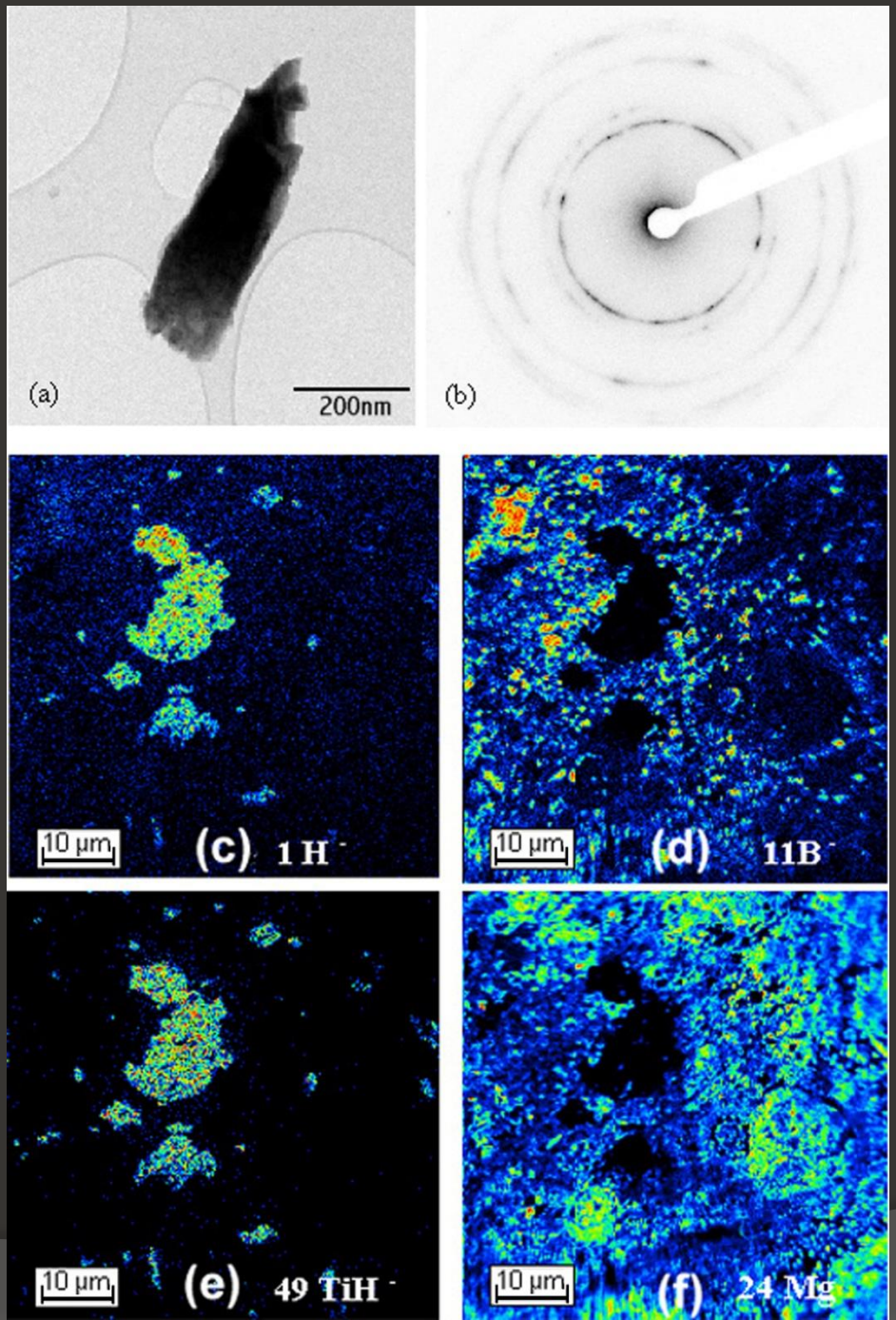

The sizes of the Ti-containing inclusions are rather big to be pinning centers by itself and randomly distributed in MgB_2

Enthalpies of formation values for a range of common Ti compounds

	Enthalpy of formation ($kJ\ mol^{-1}$)
Ti_3O_5	−2459.4
Ti_2O_3	−1520.9
TiO_2	−944.057
TiN	−336.6
TiB_2	−150 to −314
TiH_2	−15.0

a) Bright–field TEM image of a particle from a powdered sample

b) Electron diffraction pattern (contrast inverted) from the Ti-rich particle shown in (a)

(c-f) NanoSIMS ion maps of the distribution of (c) mass 1 H−, (b) mass 11 B−, (d) mass 49 TiH_2−, (e) mass 24 Mg− (f)

Evolution of MgB_2 structure with synthesis temperature increase at 2 GPa, 1 h without and with Ti additions

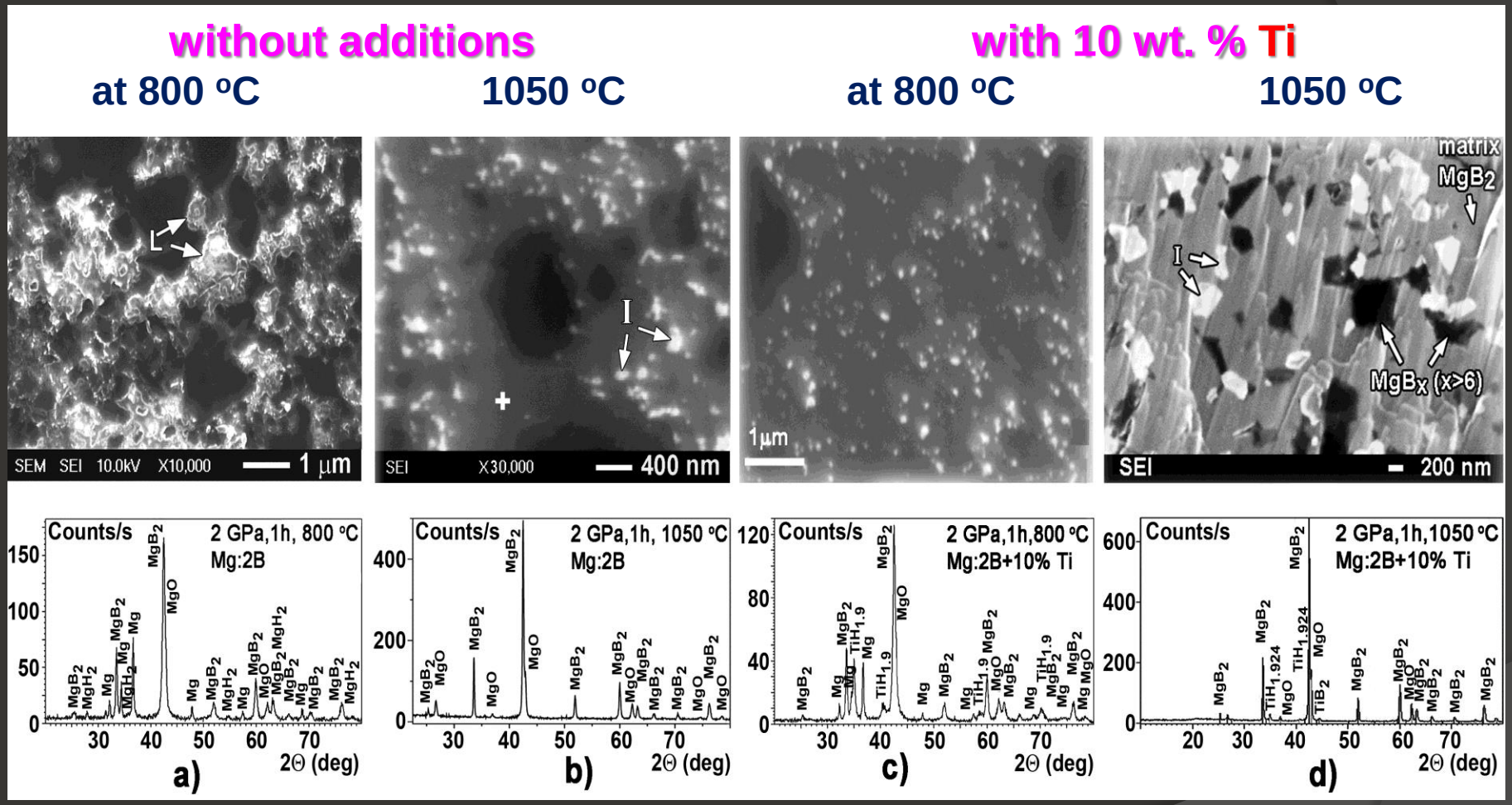

Mg-B-O nanolayers (L) → Mg-B-O inclusions (I) the most white

Mg-B-O inclusions

Mg-B-O inclusions

Modeling experiment

SEM images SEI (a) and BEI (b) of the synthesized at 2 GPa for 1 h from Mg:2B with Ti (10 wt. %, coarse grains) under 2 GPa for 1 h at 800 °C

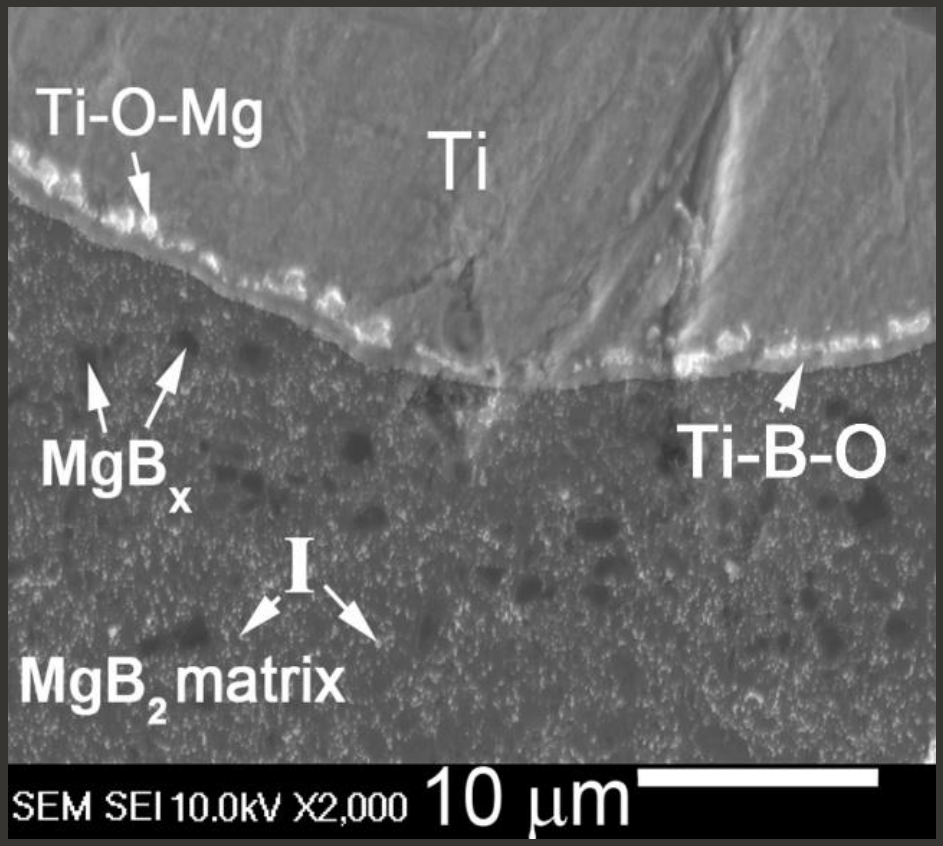

a)

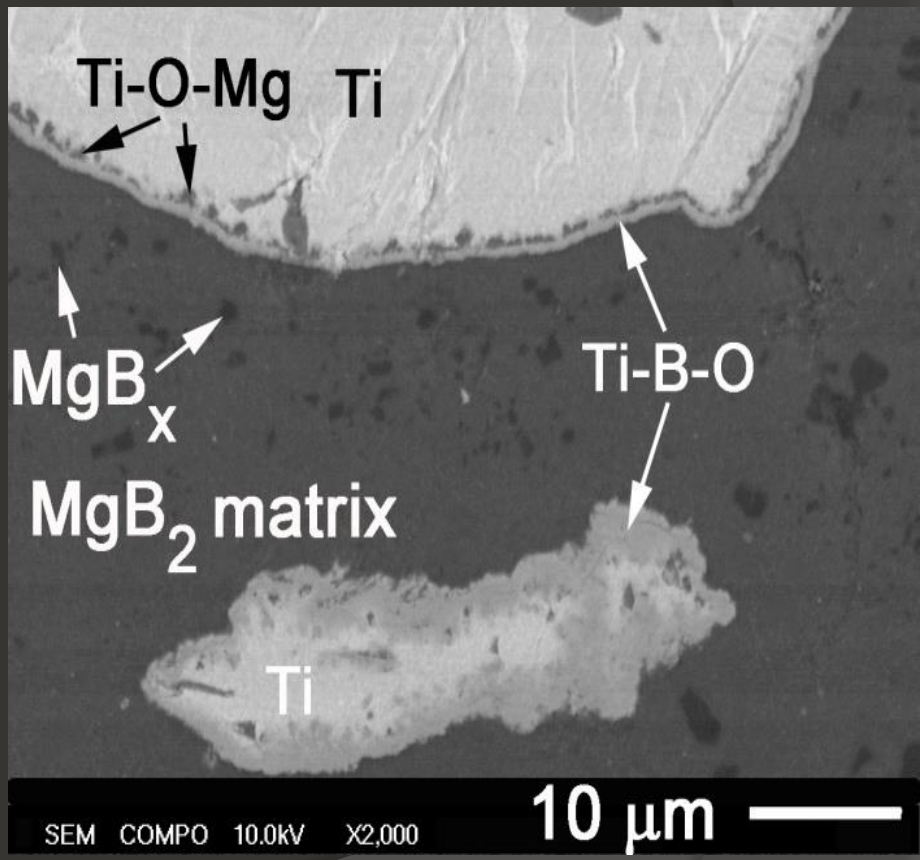

b)

Table 1. Results of quantitative Auger analysis (atomic %) made in points marked 1-6 in Fig. 2g and located at the boundary

SEM images SEI of the synthesized at 2 GPa for 1 h from Mg:2B with Ti (10 wt. %, coarse grains) under 2 GPa for 1 h at 800 °C

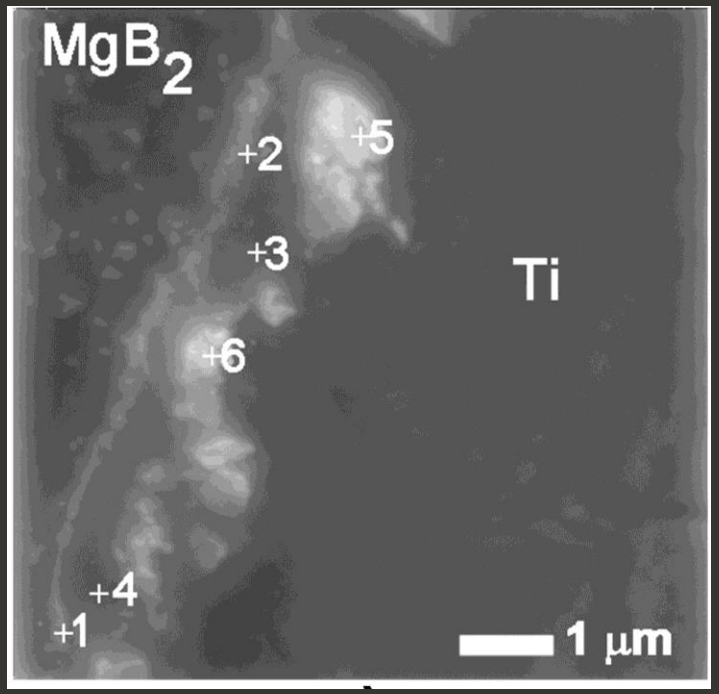

Results of quantitative Auger analysis (atomic %) made in points marked 1-6 and located at the boundary between MgB_2 and big Ti grain of the sample prepared at 2 GPa, 800 °C, 1 h. The sample was etched in Ar in the JAMP−9500F chamber before the study.

Element/ point No	B	Ti	O	Mg	C
1	22.2	10.5	33.1	22.6	11.7
2	24.5	10.8	33.1	21.2	10.3
3	41.4	31.4	8.2	3.4	15.5
4	41.3	28.2	9.1	3.2	17.7
5	4.1	13,9	44.9	29.1	8.0
6	6.5	10.1	44.8	29.1	9.4

Magnesium and oxygen enriched inclusions are observed inside the Ti grain, which were formed as a result of the Mg and O diffusion. The layer of Mg-B-O with somewhat smaller amount of oxygen (Nos 1, 2) then in inclusions (Nos. 5, 6) are well observed near to the grain boundary between the grain contained Ti. Magnesium defused into titanium more intensively than boron (compare Nos 3, 4 with Nos 5, 6, Table). **So, the redistribution of boron and oxygen in MgB_2 can be explained by a higher affinity of Ti to Mg and O than that to B.** Because of this Mg and O diffuse deeper to the Ti grain then B). We should not exclude the presence of a titanium hydride TiH_2 layer inside the Ti grain.

SEM images SEI of the synthesized at 2 GPa for 1 h from Mg:2B with Ti (10 wt. %, coarse grains) under 2 GPa for 1 h at 800 °C

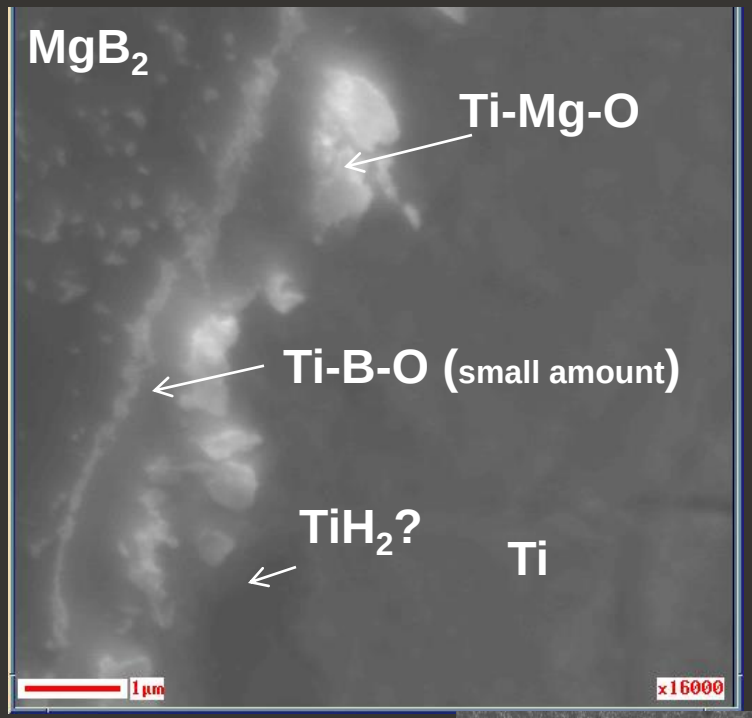

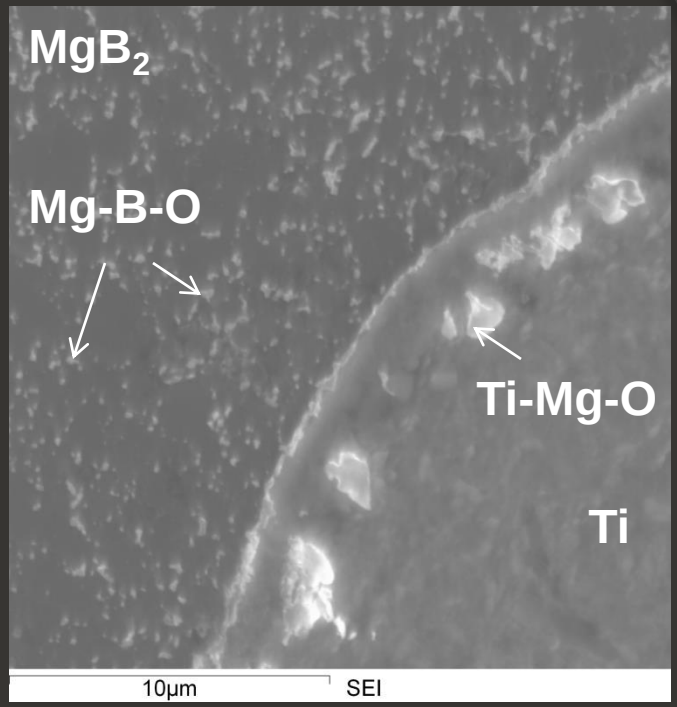

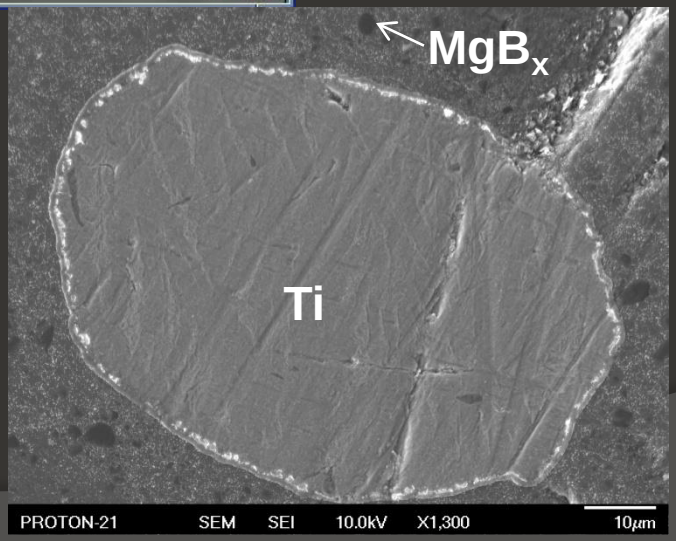

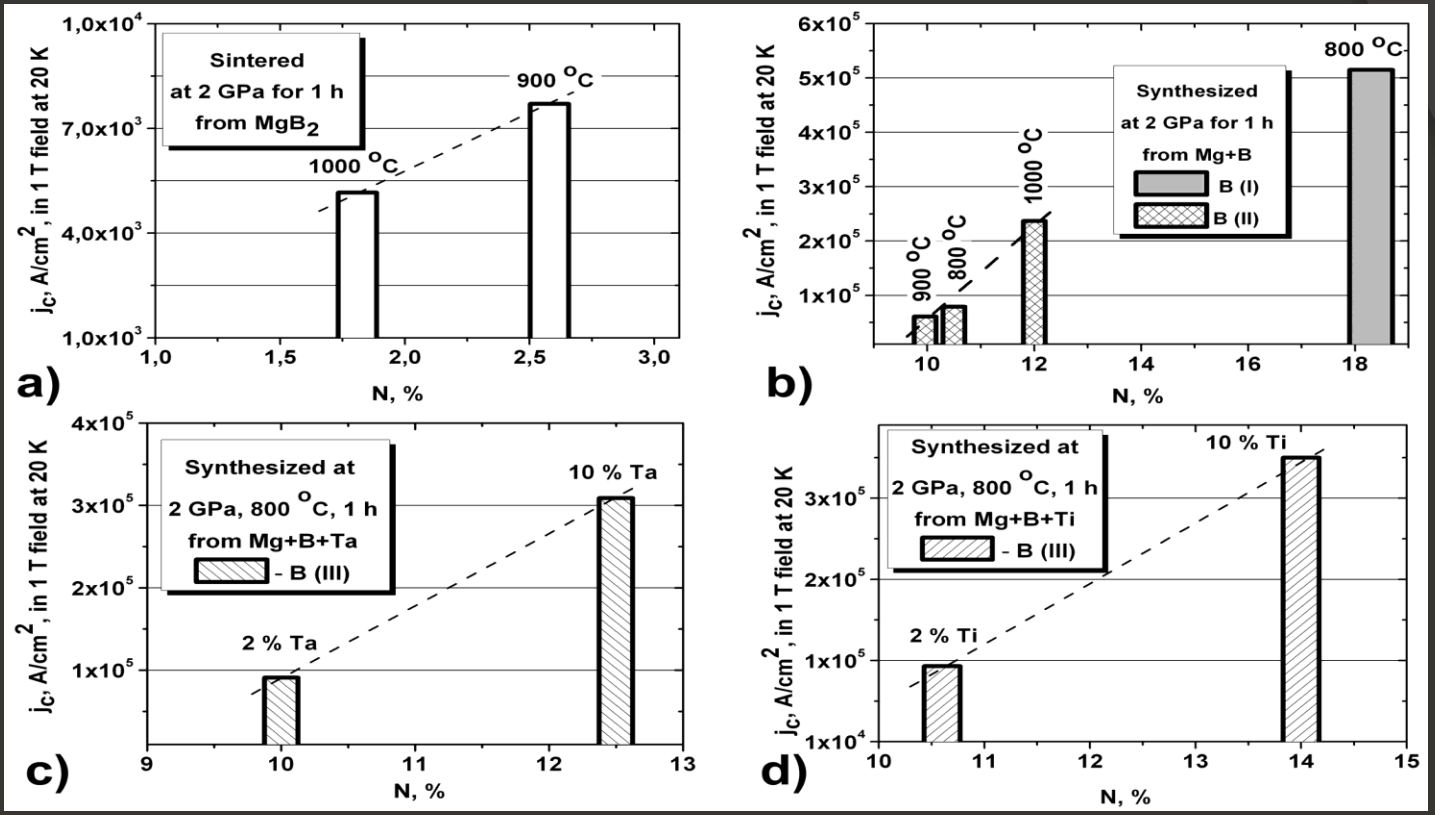

Dependences of critical current density, jc, estimated in 1T field at 20 K on the amount of "black" Mg-B (MgB12) inclusions, N, for high pressure-high temperature manufactured MgB2 samples without additions: (a) - sintered from MgB2 (7MB - 0.8 % oxygen and 10-μm grains at 1000oC and 8MB – 98% purity Alfa Aesar at 900 oC), (b)- synthesized from boron 6B (type I -1.9 % oxygen, 1.4 - μm grains) and from boron 2B (type II - 1.5 % oxygen and 4-μm grains) and (c, d) - synthesized from boron 1B (type III – 1-μm grains, MaTecK, 95-97% purity) with additions of Ta and Ti, respectively. Amount of "black" inclusions, N, was calculated as a ratio of the area occupied by "black" inclusions at the COMPO image obtained at 1600x magnification to the total area of this image

MgB_2 for fault current limiter

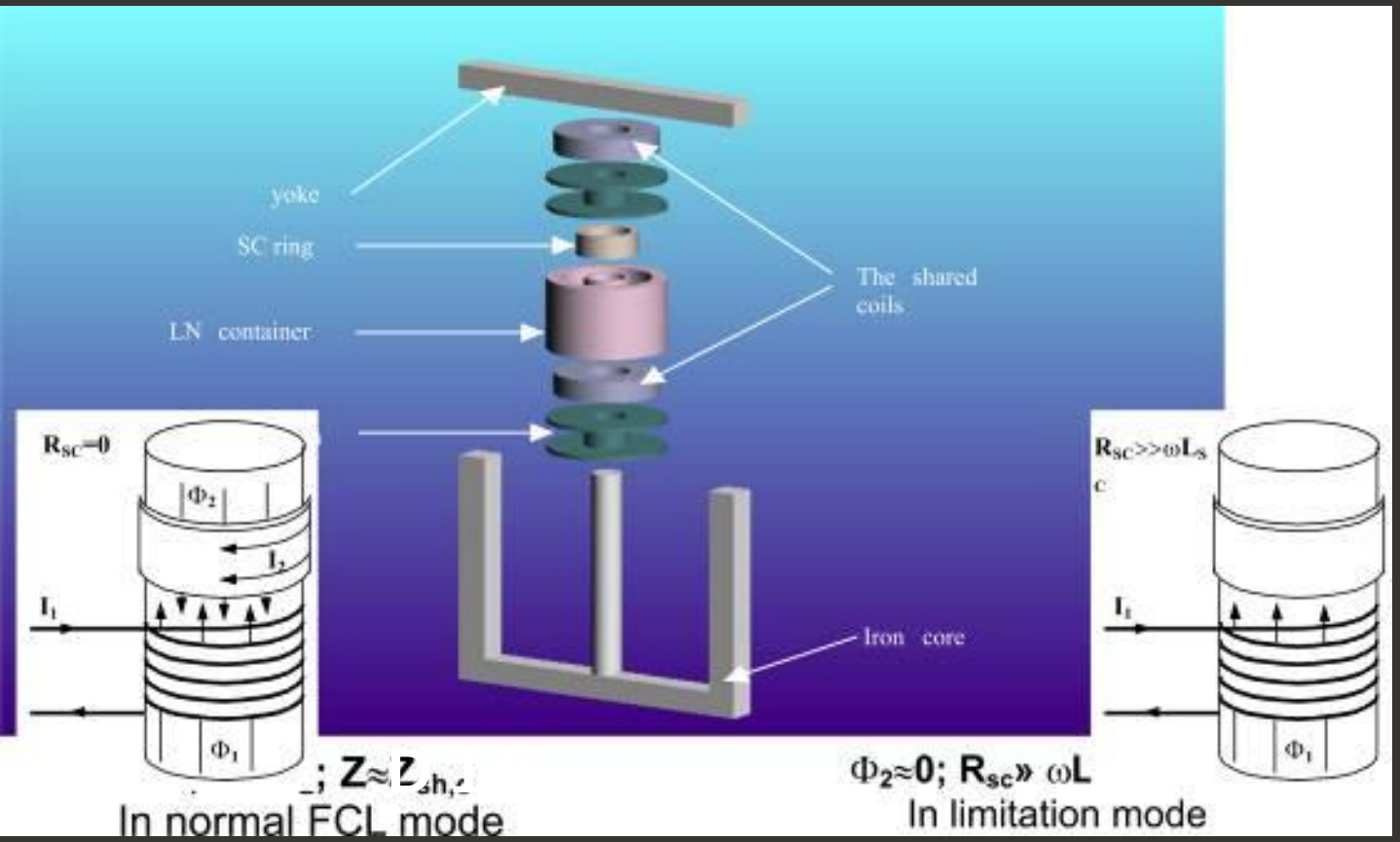

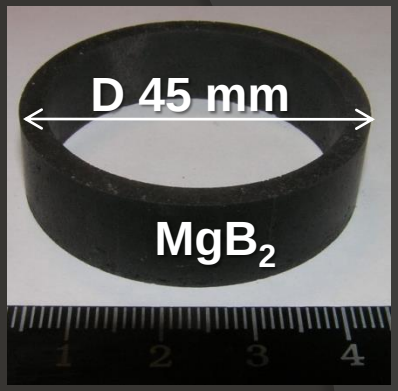

Rings cut from MgB_2 blocks

Transformer- type fault current limiter (Budapest University of Technology and Economics)

At fault event an increase in the circuit current causes a growth of the current in a superconductor higher than the critical value. The SC-or passes into the resistive state introducing a required for limitation impedance in the circuit (2–4 ms and 1 ms) .

Smart application of HP and hot-pressed MgB_2-based materials

Characteristics of the MgB2-based material synthesized at 30 MPa, 800 °C, 2 h from amorphous boron (III) (H.C. Starck, 1.5 % O, 4 μm grains) and magnesium (I) taken in the MgB_2 stoichiometry and of the ring cut from this material:

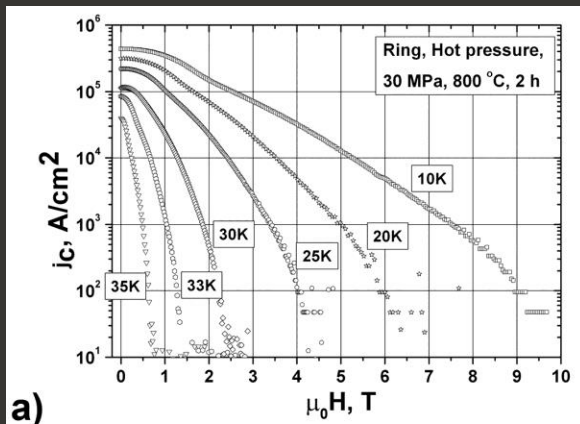

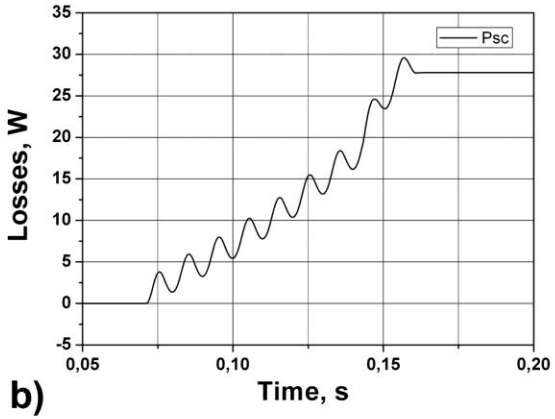

Quenching current 24000 A.

j_c= 63200 A/cm².

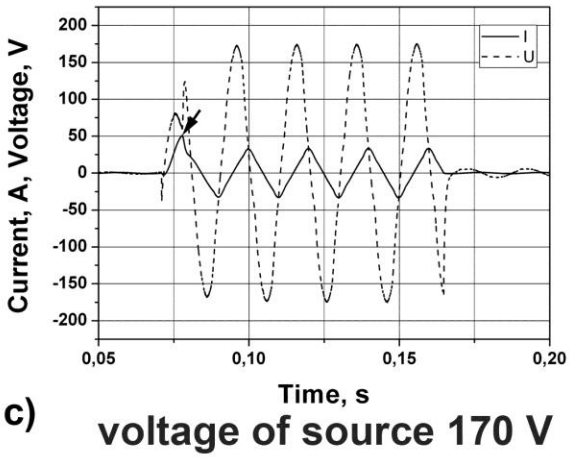

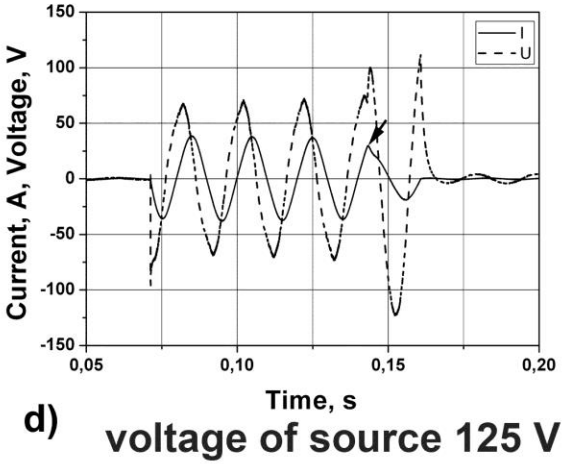

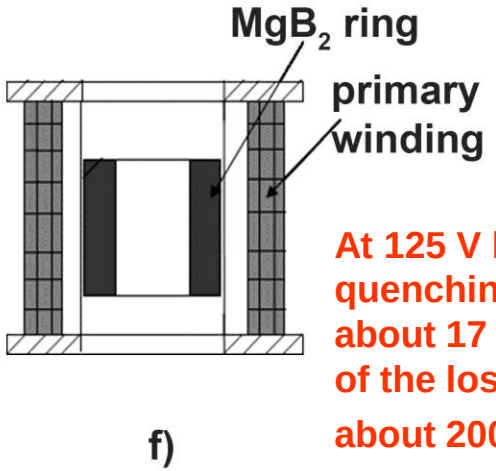

At 125 V losses till quenching are about 17 J. Power of the losses is about 200 W.

Typical oscilloscope traces of the current (solid lines) and voltage drop across the primary normal-metal winding (dashed lines) at 4.2 K. Arrows show the quenching current. Voltage of source was 170 V (c) and 125 V (d);
e) ring: outer diameter – 45 mm, height - 11.6 mm, wall thickness – 3.3 mm.

First MgB2-based 1.3 kW motor by MAI (Moscow) , IPHT (Jena), ISM NASU, Kiev

Experimental HTS Motor for 20 K Temperature

Cross-section of HTS Motor

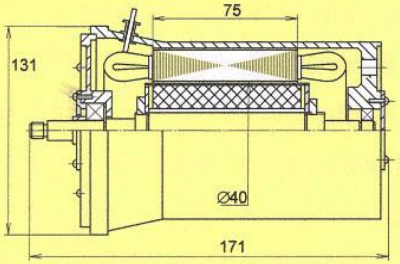

General View of HTS Motor

Compound HTS-Ferromagnetic Rotor With YBCO Bulk Elements

General View of YBCO Samples

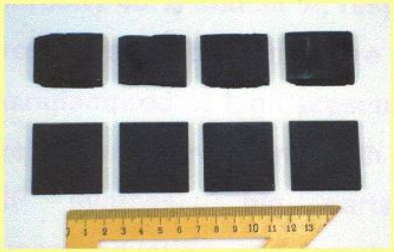

Rotor With YBCO Bulks

Compound HTS-Ferromagnetic Rotor With MgB_2 Bulk Elements

General View of MgB_2 Bulk Samples

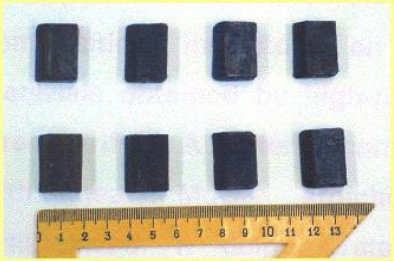

Rotor With MgB_2 Samples

Test results of reluctance motor with MgB_2 blocks

Temperature: T = 15 … 20 K

Phase voltage: U = 120 V

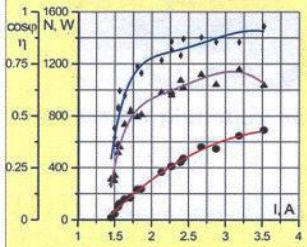

Phase voltage: U = 160 V

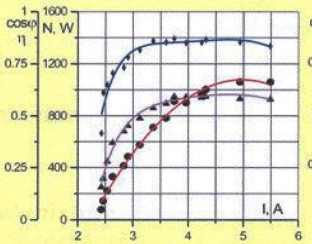

Phase voltage: U = 210 V

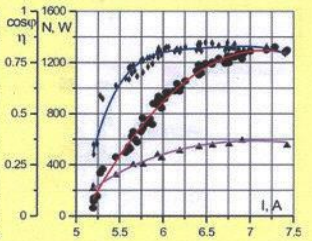

◆ - efficiency, ● - output power, ▲ - power factor

Test results of reluctance motor with YBCO blocks

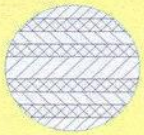

Temperature: T = 15 … 20 K

Phase voltage: U = 120 V

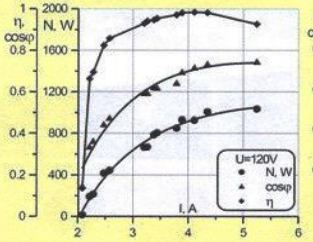

Phase voltage: U = 160 V

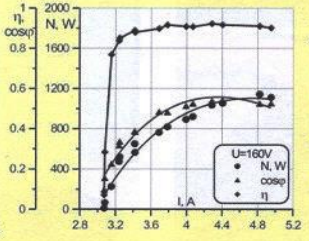

Phase voltage: U = 215 V

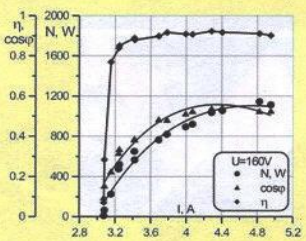

◆ - efficiency, ● - output power, ▲ - power factor

Conclusions

- The distribution of nanostructural inhomogeneities, such as areas with a high concentration of B and impurity O, plays a key role in the variation of j_c in MgB_2 materials.
- Auger and SEM studies show that with increasing manufacturing temperature oxygen enriched 15-20 nm thick nano-layers transform into distinct dispersed Mg-B-O inclusions.
- In parallel, the Ti addition results in a further increase in j_c , because Ti fosters the localization (or segregation) of oxygen and of higher magnesium borides and facilitates the formation of a homogeneous MgB_2 matrix with low oxygen content, but with Mg-B-O and MgB_x pinning centers.
- At low synthesis temperature Ti can absorb hydrogen forming titanium hydrides, thus preventing the formation of MgH_2 and promoting the material densification.
- The positive effect of Ti addition results from the high ability of Ti to absorb H, O, and Mg.

Thank you for your kind attention!

Stucture of MgB_2 with 10 wt% of Ti synthesized at 2 GPa, 800 °C, 1 h

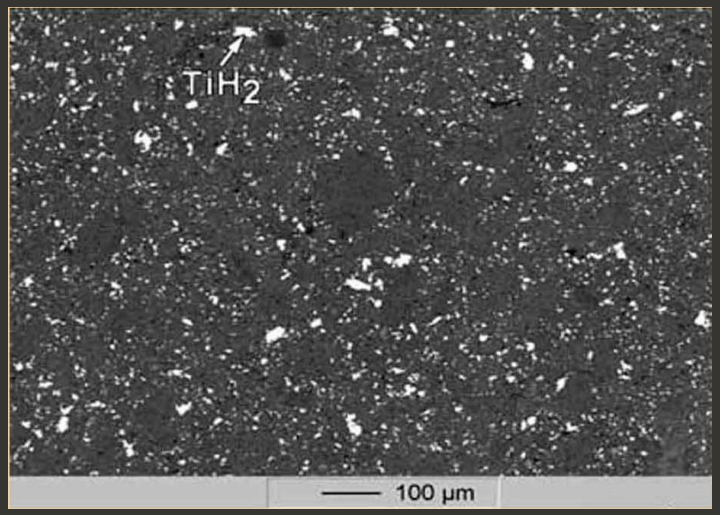

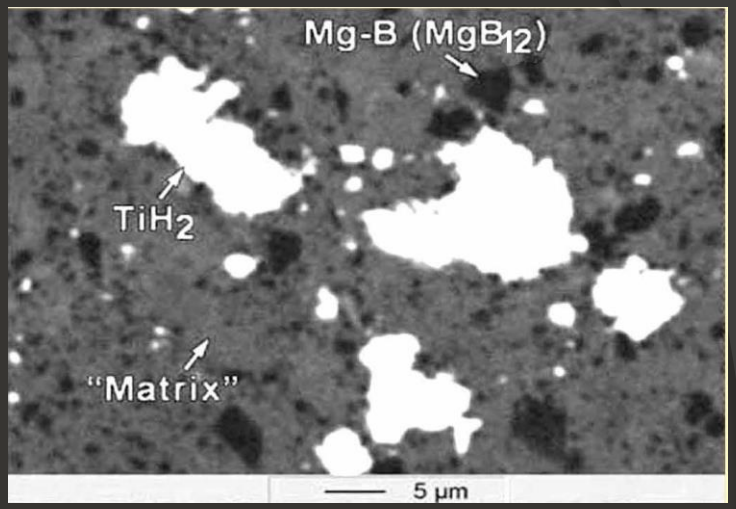

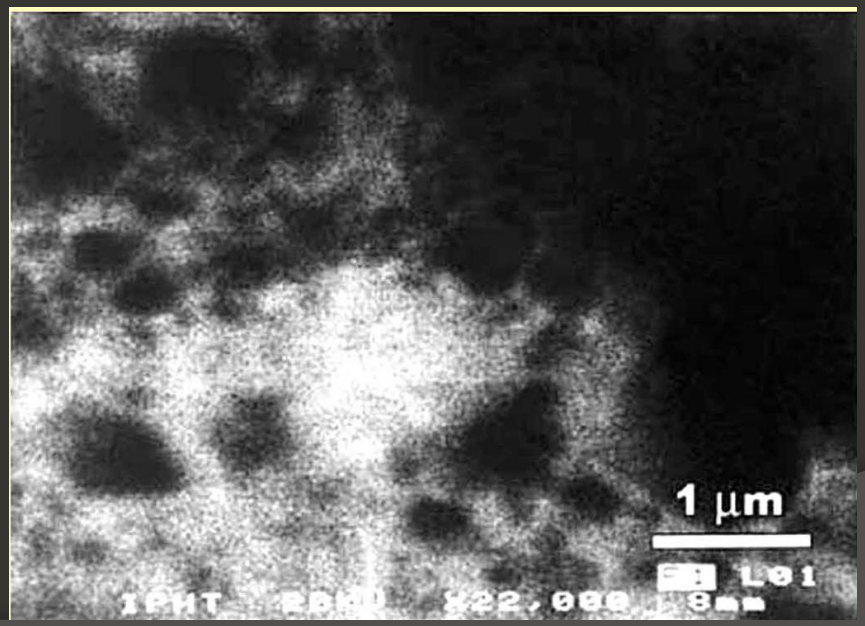

SEM (COMPO)

Pressure 30- 50 MPa can not totally suppress the volatility of Mg, thus MgB_{4-6} porous regions are forming

***Spark plasma sintering (SPS):* 50 MPa, 1050 ^{o}C, 32 min**

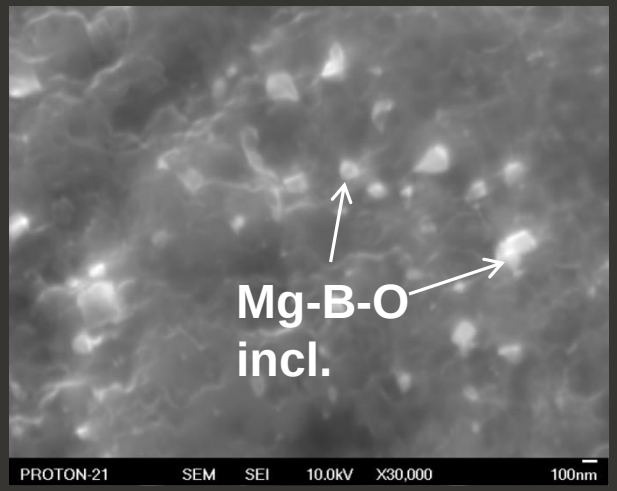

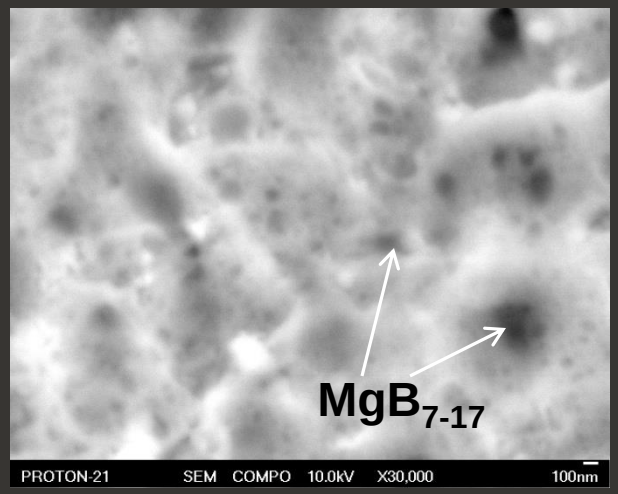

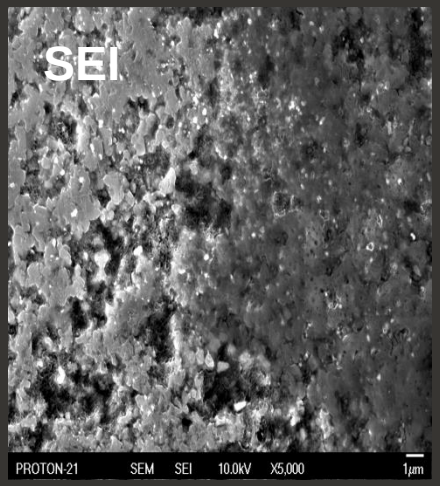

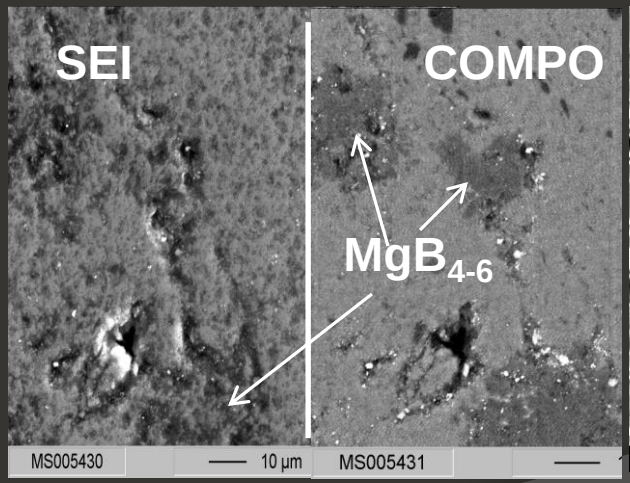

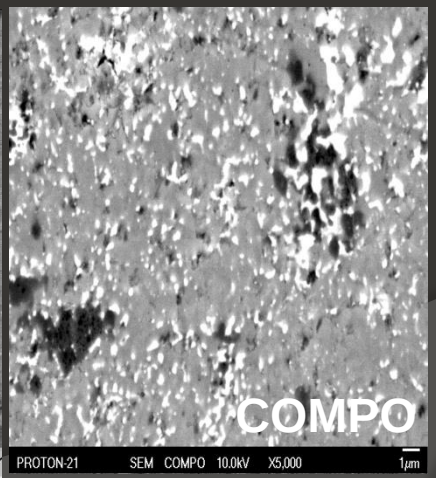

***in-situ* form Mg:2B**

***ex-situ* form MgB_2**

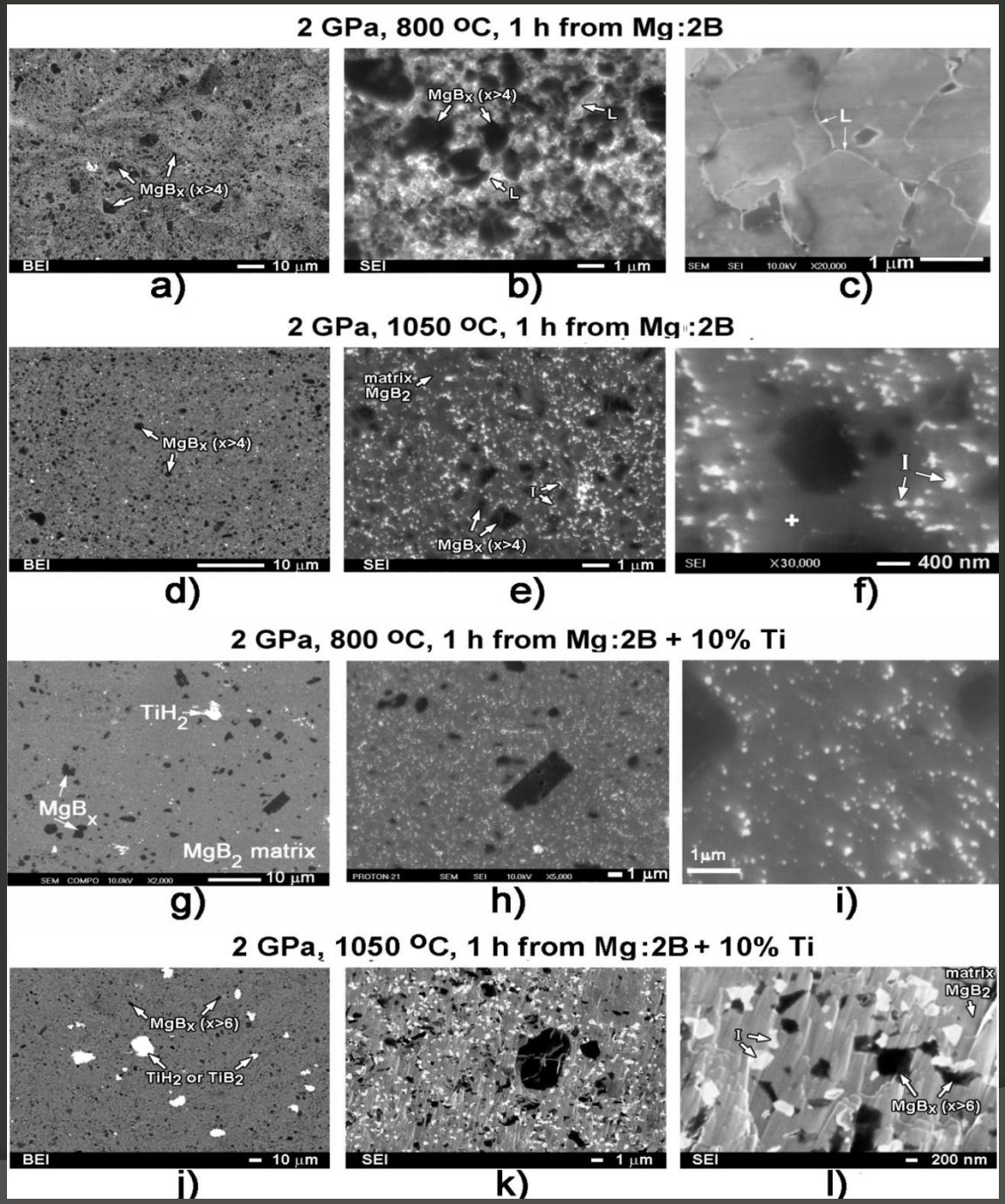

Mg:2B, 2 GPa, 800 °C, 1 h

Mg:2B, 2 GPa, 1050 °C, 1 h

Mg:2B + Ti (10 wt.%)
2 GPa, 800 °C, 1 h

Mg:2B + Ti (10 wt.%)
2 GPa, 1050 °C, 1 h

The amount of "black" MgB_x inclusions, N, for high pressure synthesized MgB_2 without additions and with additions of Ta and Ti N,%, was calculated as a ratio of the area that is occupied by "black" inclusions in the image of the structure obtained at 1600x magnification to the total area of the image obtained by SEM in the BEI mode.

The amount of "black" MgB_x inclusions, N, decreased by 6% by increasing the temperature from 800 up to 950 ^oC (from 1.8 to 8%)

The addition of Ti led to a further increase of MgB_x inclusions. If the Ti addition increased from 2 to 8 wt. % the amount of "black" MgB_x inclusions increased by about 6% as well .

Despite the essentially different structures and properties, the MgB_x (x>4) inclusions are practically "invisible" for a traditional x-ray diffraction analysis. This can be caused by their fine dispersion in the material structure and the large number of atoms in the unit cell of low symmetry resulting in many "reflecting planes", which essentially reduce the intensities of the x-ray reflections as compared to those of the MgB_2 matrix having a simple hexagonal unit cell

With manufacturing temperature increase the critical current density Increased in low and medium magnetic fields

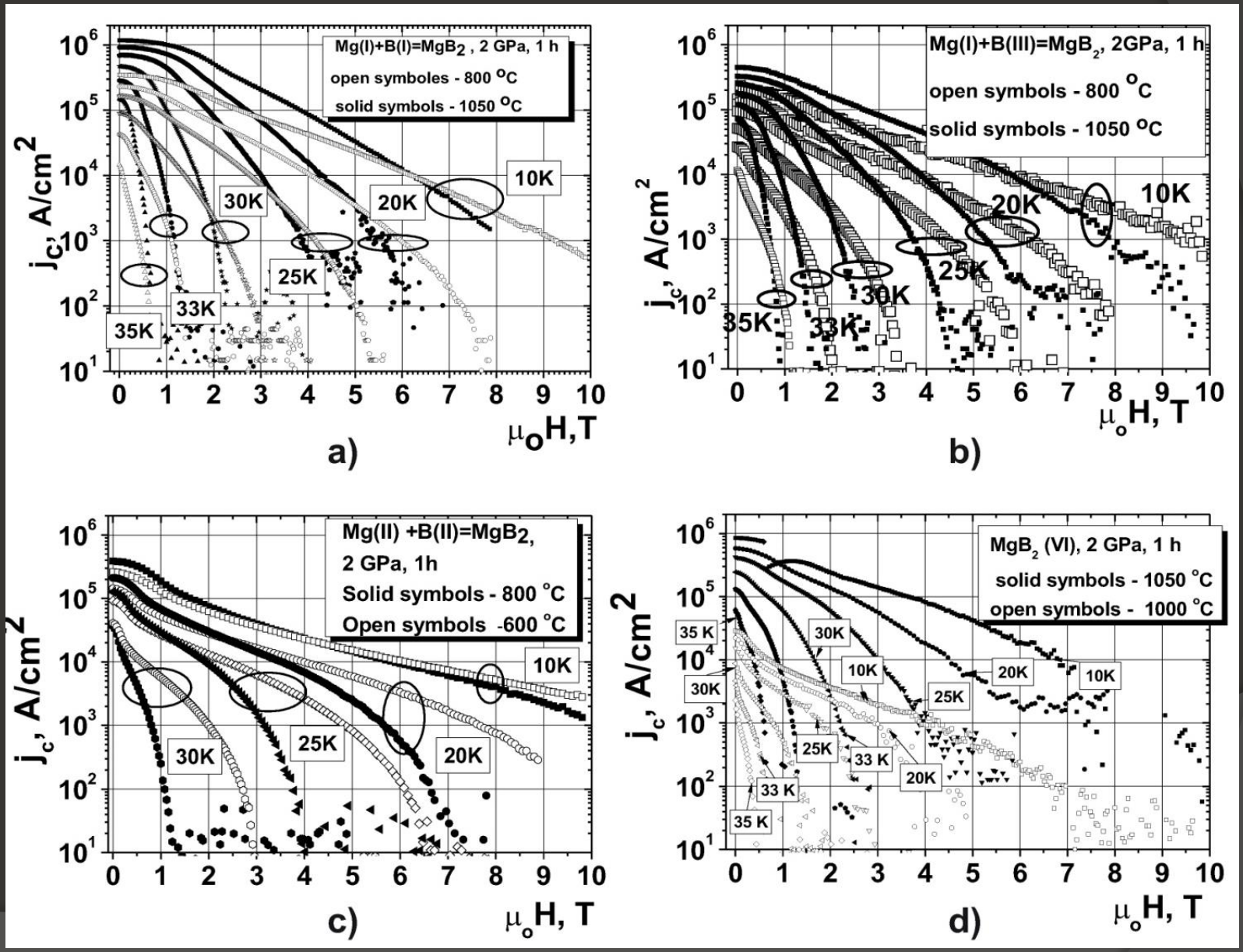

Experimental

2 GPa - HP, 30 MPa- HotP, 50 MPa – SPS, 0.1 MPa Ar - PL

Initial materials

(I) *in-situ* from Mg:B=1:2 (MgB_2) , from Mg:B=1:7 and 1:12 mixing and milling in a high speed activator for 3-5 min

- ✓ Boron (B) amorphous

Characteristics of initial boron powders.

Type of B	Grain size	O, wt%	C, wt%	N, wt%	H, wt%
I	<5 μm	0.66	0.31	0.48	0.32
II	<1 μm	-	3.5	1.02	0.87
III	4 μm	1.5	0.47	0.40	0.37

- ✓ Magnesium (Mg)

  Mg(I) turning (Technical Specifications of Ukraine 48-10-93-88)

  Mg(II) powder 325 mesh (HyperTec, USA)

(II) *ex-situ* from MgB_2 powder

- ✓ Magnesium diboride (98% purity)

Intermediate conclusions

With the manufacturing temperature increase the oxygen-enriched nanolayers "L" (15-20 nm thick) transformed into separate inclusions "I" and the sizes and amount of MgB_x inclusions are essentially reduced, what was observed in the range of 0.1 MPa - 2 GPa pressures.

But in the case of processing under 0.1 MPa (PL) the X-ray diffraction patterns showed that materials manufactured at 1050 ^oC for 15 min have MgB_4 structure and after 2 h – MgB_7.

The contradiction between the results of X-ray diffraction analysis and SEM –Auger study can be explained by formation of the solid solutions of boron in MgO and of oxygen in MgB_2 and what due to the similarity of the scattering ability cannot be detected by traditional X-ray diffraction.

Pressure effect on MgB_2

Dependencies of critical current density, j_c, vs. magnetic field, B

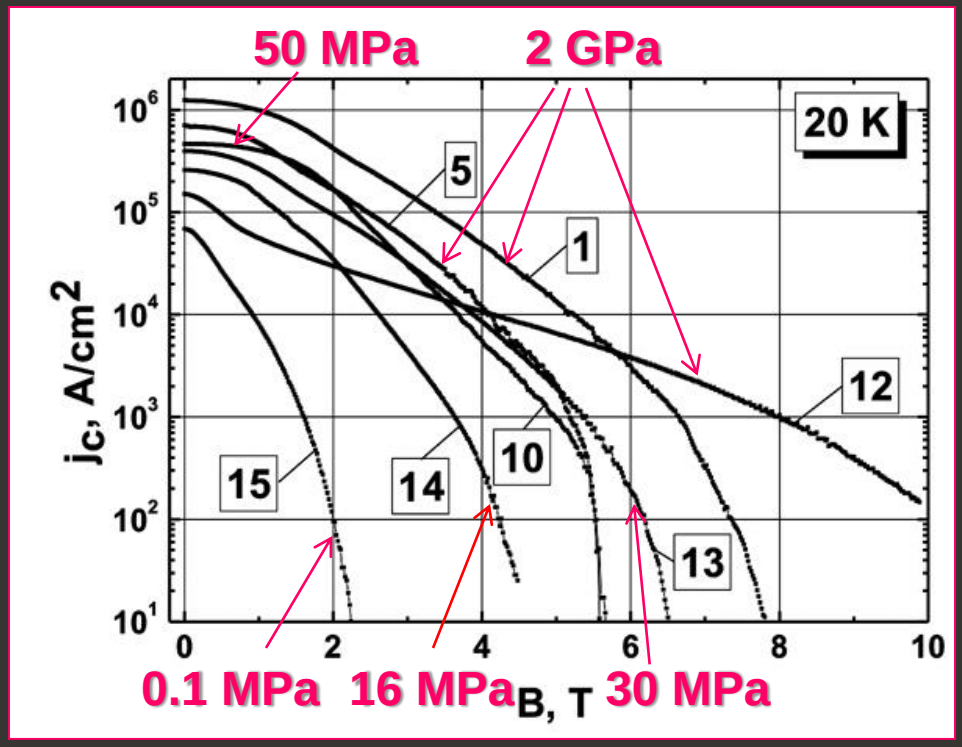

Corresponding dependencies of volume pinning force Fp(n), vs. magnetic field, B

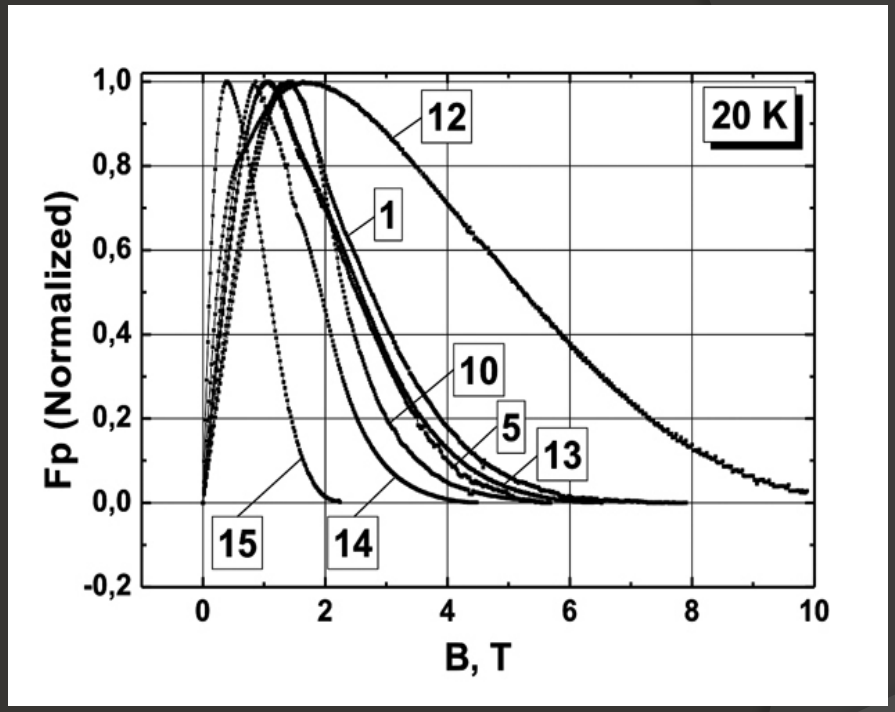

Curves: (1) Mg(I):2B(I)+10% SiC, 2GPa, 1050 °C,);
(5) Mg(I):2B(III)+10% Ti, 2 GPa, 1050 °C, 1 h,);
(10) Mg(I):2B(III, 50 MPa (SPS), 600°C- 0.3 h, 1050 °C-0.5 h,
(12) Mg(II):2B(II) with 3.5 % C, 2 GPa, 600 °C, 1 h,
(13) Mg(I):2B(III)+10% Ti, 30 MPa ,550°C- 1 h, 1000 °C- 0.2 h);
(14) MgB_2, 16 MPa (SPS), 1150 °C, 0.3 h,);
(15) Mg(I):2B(III), 0.1 MPa, Ar, 800 °C, 4 h,

The distribution of boron and impurity oxygen in the MgB_2 structure is of high importance for attaining high jc . Rather high amount of impurity oxygen can be present in the materials with high SC characteristics.

MgB_2 (Mg(I):2B(III), 2 GPa, 1200 °C, 1h), 76 wt % MgB_2, 24 wt % MgO

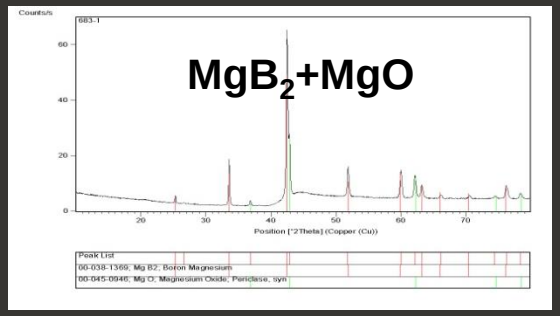

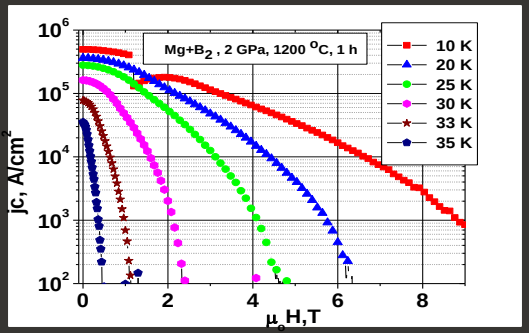

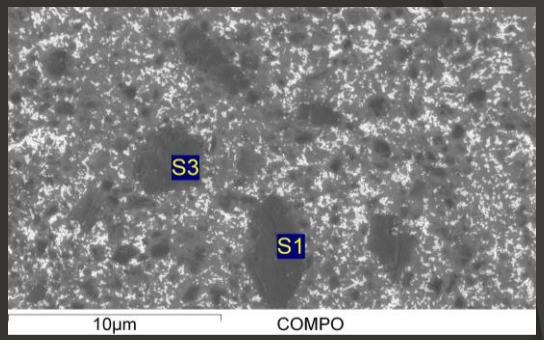

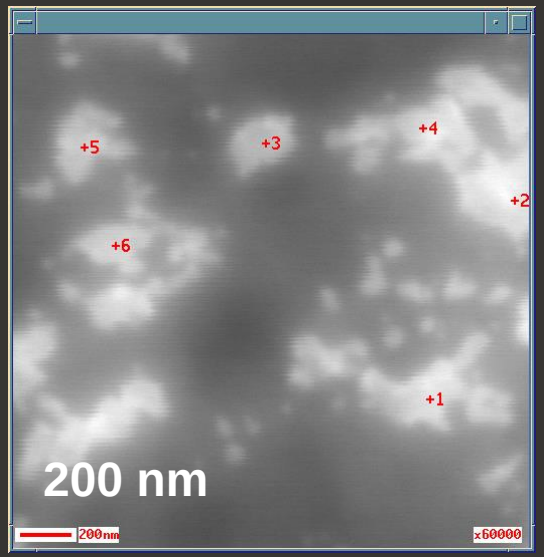

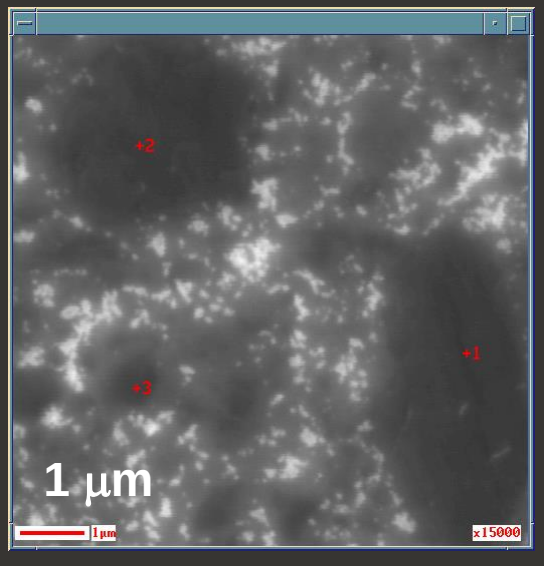

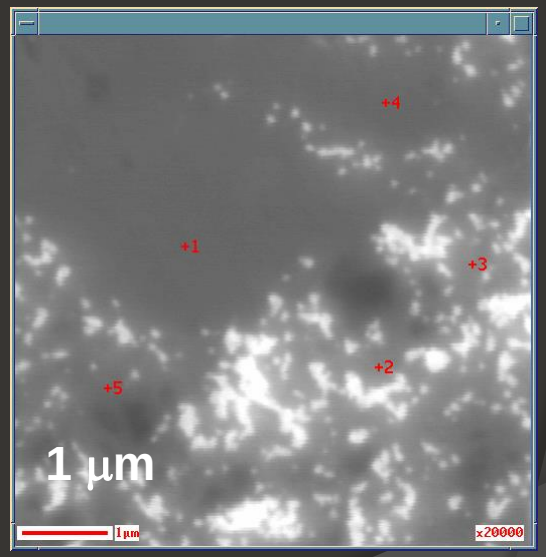

Atom %

S-007	B	O	Mg	Total
1	46,7	26,2	27,1	100,0
2	45,4	27,2	27,4	100,0
3	51,6	24,6	23,7	100,0
4	49,1	26,2	24,7	100,0
5	43,2	28,7	28,1	100,0
6	46,1	28,1	25,8	100,0

Atom %

S-009	B	O	Mg	Total
1	91,6	1,3	7,0	100,0
2	91,8	2,1	6,1	100,0
3	90,9	3,6	5,5	100,0

Atom %

S-011	B	O	Mg	Total	B/Mg
1	63,6	7,8	28,6	100,0	**2,22**
2	55,6	15,5	28,9	100,0	**1,92**
3	51,7	17,9	30,4	100,0	**1,70**
4	56,0	15,1	28,9	100,0	**1,93**
5	53,5	16,9	29,6	100,0	**1,81**

SEM structures

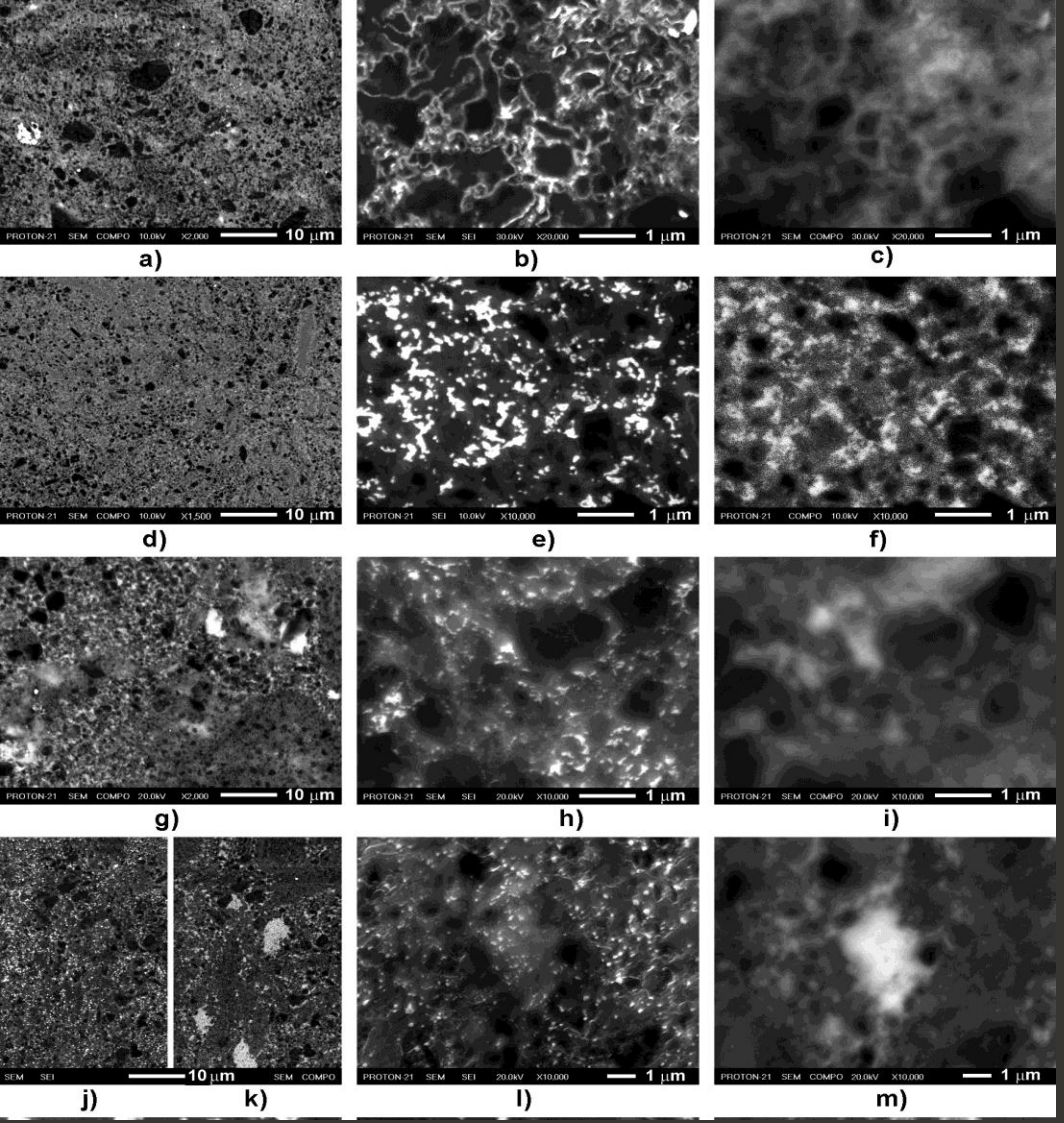

Mg:2B
2 GPa, 800 °C, 1 h

Mg:2B
2 GPa, 1050 °C, 1 h

Mg:2B
2 GPa, 800 °C, 1 h, +10%SiC

Mg:2B
2 GPa, 1050 °C, 1 h, +10%SiC

Mg:2B
1050°C

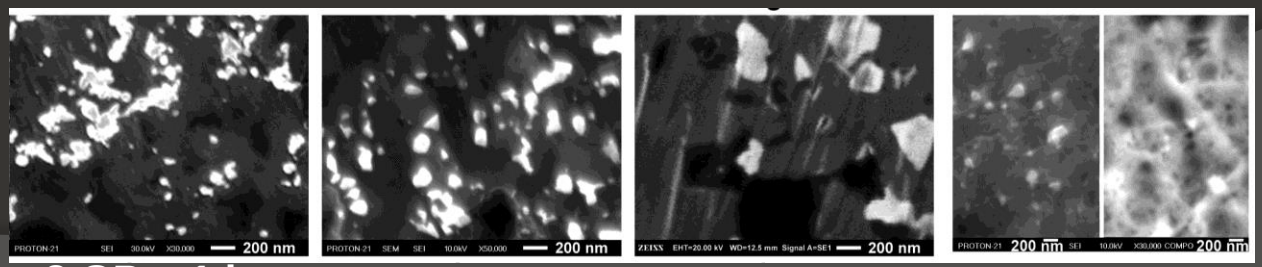

2 GPa, 1 h **2 GPa, 1 h,+SiC** **2 GPa, 1 h,+Ti** **50 MPa, 1 h, SPS**